NASA CR-134712
PWA™-5022

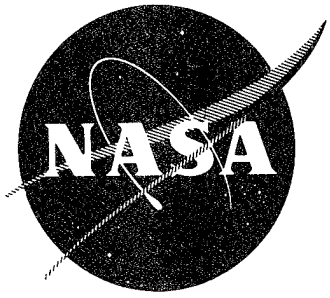

IMPACT RESISTANCE OF HYBRID COMPOSITE FAN BLADE MATERIALS

by L. A. Friedrich

Pratt & Whitney Aircraft
Division of United Aircraft Corporation

prepared for

National Aeronautics and Space Administration

NASA Lewis Research Center

Contract NAS3-17789

1. Report No.	2. Government Accession No.	3. Recipient's Catalog No.
NASA CR-134712		

4. Title and Subtitle	5. Report Date
IMPACT RESISTANCE OF HYBRID COMPOSITE FAN BLADE MATERIALS	May 1974
	6. Performing Organization Code
7. Author(s)	8. Performing Organization Report No.
L. A. Friedrich	PWA™ 5022
	10. Work Unit No.
9. Performing Organization Name and Address	
Pratt & Whitney Aircraft Division of United Aircraft Corporation East Hartford, Connecticut	11. Contract or Grant No. NAS3-17789
	13. Type of Report and Period Covered
12. Sponsoring Agency Name and Address	Contractor Report
National Aeronautics and Space Administration Washington, D. C. 20546	14. Sponsoring Agency Code

15. Supplementary Notes

Project Manager, Robert H. Johns, Materials and Structures Division
NASA Lewis Research Center

16. Abstract

Improved resistance to foreign object damage was demonstrated for hybrid composite simulated blade specimens. Transply metallic reinforcement offered additional improvement in resistance to gelatin projectile impacts. Metallic leading edge protection permitted equivalent-to-titanium performance of the hybrid composite simulated blade specimen for impacts with 1.27 cm and 2.54 cm (0.50 and 1.00 inch) diameter gelatin spheres.

17. Key Words (Suggested by Author(s))	18. Distribution Statement
Composite Materials Impact Foreign Object Damage (FOD) Hybrid Composites	Unclassified - Unlimited

19. Security Classif. (of this report)	20. Security Classif. (of this page)	21. No. of Pages	22. Price*
Unclassified	Unclassified	58	3.00

* For sale by the National Technical Information Service, Springfield, Virginia 22151

FOREWORD

This report describes the work accomplished under Contract NAS3-17789 by the Pratt & Whitney Aircraft Division of United Aircraft Corporation for the Lewis Research Center of the National Aeronautics and Space Administration during the period July 1973 to April 1974.

Mr. Robert H. Johns of the Materials and Structures Division of the Lewis Research Center was the Project Manager for NASA. Mr. Leonard A. Friedrich was the Program Manager for Pratt & Whitney Aircraft. Mr. H. Belanger conducted the bench ballistic testing and Mr. J. Graff of the Hamilton Standard Division of United Aircraft Corporation conducted the spin impact testing reported.

TABLE OF CONTENTS

LIST OF ILLUSTRATIONS

LIST OF ILLUSTRATIONS (Cont'd)

LIST OF ILLUSTRATIONS (Cont'd)

IMPACT RESISTANCE OF HYBRID COMPOSITE FAN BLADE MATERIALS

L. A. Friedrich

I. SUMMARY

Impact testing of panels using 1.27 cm diameter gelatin projectiles indicated that adding up to 40% S-glass reinforcement to Type II graphite epoxy composite material improves resistance to penetration and delamination. The 0°, ±45° and 0°, ±22° configurations appeared to be superior to 0°, 90°, ±45° configurations.

Ballistic testing of simulated blade specimens with 2.54 cm diameter gelatin projectiles complemented the panel ballistic data. Loss of torsional rigidity proved to be an effective method for quantitatively assessing damage caused by ballistic impact. The test data indicated that both the 0°, ±45° orientation and 0°, ±22° orientation were superior in resisting impact damage to the 0°, 90°, ±45° orientation. The 0°, ±22° specimens suffered trailing edge tip splitting – a failure mode unique to this construction.

As measured by loss of torsional rigidity, trans-ply metallic reinforcement demonstrated improved ballistic impact resistance in blade specimen testing.

Metallic leading edge protection provided equivalent to titanium blade specimen impact resistance in 1.27 cm and 2.54 cm diameter gelatin projectile impact testing.

Spin impact testing resulted in less severe damage than bench impact testing. The absence of high speed motion pictures of the spin impact tests precluded a definite conclusion as to whether comparable impacts had occurred in both the spin and bench tests.

Testing of four thicknesses of blade specimens with three sizes of gelatin projectiles provided data to establish a tentative relation between the necessary blade thickness to resist impact and the mass, velocity and angle of impingement of foreign objects.

II. INTRODUCTION

Fiber composite fan blades have the potential to reduce the weight and improve the performance of advanced turbofan engines. The major technical problem associated with composite material fan blades is their lack of impact resistance to ingested foreign objects. In order to take full advantage of fiber composite material, an expanded technology base is required for the design of composite blades which will operate safely when subjected to impact by foreign objects.

Data reported previously (Reference 1), have provided a basis for understanding the performance of composite material blades under impact conditions. This data indicated that improvements in the resistance of composite material blades to foreign object damage can be achieved by using materials with improved transverse properties, multi-type fiber reinforced (hybrid) composites and optimum filament orientation.

The objective of the current program was to determine the relative impact resistance of homogeneous graphite fiber and hybrid composite materials. The effect of layup angles, stacking sequence, and composition was investigated.

Flat panels of Type II graphite fiber and hybrid composites of Type II graphite and S-glass were fabricated and tested ballistically at varying velocities using gelatin projectiles to determine the relative impact resistance.

Blade specimens were fabricated with varied ply orientation and proportions of Type II graphite and S-glass and ballistically tested, complementing the work on flat panels. The effects of blade specimen thickness, trans-ply metal reinforcement and metal leading edge protection under varying mass and velocity gelatin projectile impacts were also investigated. Both static and spin impact testing have been used in evaluating the resistance of composite blade specimens and titanium alloy blade specimens to ballistic damage.

III. TEST PROGRAM

A. RAW MATERIAL QUALITY ASSURANCE

The composite materials used in this program were 7.6 cm wide epoxy prepreg fiber tape purchased from the 3M Company. These tapes included the graphite system, Modmor II/ PR 286, and S-Glass/PR 286. Visual inspection indicated that the tape material had good collimation of filaments and was uniform. Gel time, volatile content and fiber content were determined (Table I). These characteristics are consistent with both vendor supplied data and limits established in prior work and are uniform throughout the materials tested.

TABLE I

QUALITY TESTING OF PREPREG MATERIAL

FIBER/RESIN	VOLATILES* (%)	149°C GEL TIME MIN	WEIGHT PERCENT FIBER
S-Glass/PR-286			
Lot 42	0.4	14.7	61.6
Lot 56	0.3	15.3	65.7
Modmor II/PR-286			
Lot 547	0.7	12.7	62.2
Lot 551	0.3	14.5	62.3

*Exposed for 30 minutes at 149°C.

B. MECHANICAL PROPERTY CHARACTERIZATION

Unidirectional laminates of graphite/epoxy, S-glass/epoxy and the hybrid systems considered in this program were fabricated to provide material for mechanical property characterization. The panels were inspected by ultrasonic "C" scan techniques, density measurement and acid digestion to determine void content and fiber volume. All parts were of good quality with fiber volume 57 ±2% and less than 2% void content.

Test specimens used in measuring mechanical properties were as follows:

- Longitudinal tension: straight-sided rectangular bar, 20.3 cm long x 0.635 cm wide x 0.127 cm thick; fiberglass doublers bonded on each end.
- Transverse tension: straight-sided rectangular bar, 10.2 cm long x 1.27 cm wide x 0.127 cm thick; fiberglass doublers bonded on each end.
- Short beam shear: 1.27 cm long x 0.635 cm wide x 0.254 cm thick; span-to-depth ratio of 4:1.
- Charpy impact: square bar 1.0 cm x 1.0 cm x 5.5 cm with a 45° V-notch.
- Longitudinal flexural: straight-side rectangular bar, 12.7 cm long x 1.27 cm wide x 0.254 cm thick. Four-point loading was used to measure strength and modulus.

The mechanical property data are presented in Table II.

A review of this data indicates that, as expected, increasing fiberglass content lowers the modulus of the laminates and increases the Charpy impact strength providing a basis for expected improvement of composite FOD resistance for hybrid laminates.

TABLE II

MECHANICAL PROPERTIES OF PR-286 UNIDIRECTIONAL COMPOSITES
(Values Represent Average of Two Tests at 20°C)

	HYBRID SYSTEMS			
Property	A All Graphite	B 80% Graphite 20% S-Glass	C 60% Graphite 40% S-Glass	All Glass
Composite Density, g/cc	1.53	1.62	1.67	1.99
Longitudinal Tensile Strength, GN/m^2	1.16	1.23	1.02	1.50
Longitudinal Tensile Modulus, GN/m^2	141	140	117	50.0
Longitudinal Flexural Strength, GN/m^2	1.35	1.14	0.95	> 0.84[1]
Longitudinal Flexural Modulus, GN/m^2	155	130	100	43.0[1]
Short Beam Shear Strength (L/D : 4/1), MN/m^2	82.7	84.1	93.8	91.7
Transverse Tensile Strength, MN/m^2	26.7	42.1	62.1	89.6
Transverse Tensile Modulus, GN/m^2	10.9	7.9	9.7	22.1
Notched-Charpy Impact Strength, Joules	7.8	19.3	27.9	47.5

Legend: 1) 48 v/o fiber content specimens; others 57 ±2%

C. PANEL IMPACT STUDIES

Impact testing of flat panel specimens conducted during a previous program (Reference 1) indicated that gelatin ball projectiles used to simulate birds ingested by turbine engines, rather than ice or steel projectiles, caused the most severe damage to composite materials. Therefore the gelatin projectiles were selected for use in the ballistic testing in this effort.

Testing had also indicated that a dispersed ply configuration - where the angle ply material was distributed through the entire section of the specimen rather than localized on the surface- resulted in improved impact resistance. Thus dispersed ply lay-ups were used in the construction of all test specimens.

To continue to build on the data base provided in the referenced program, ballistic testing was conducted on flat panel specimens to establish the threshold velocity to cause damage as related to ply orientation and the relative proportions of graphite and S-glass fiber.

1. Fabrication

Panels 267 x 267 mm and 114 x 267 mm made up of 20 plies were compression molded at 138°C for 120 minutes to a nominal final thickness of 2.6 mm. These panels were then machined into 230 x 50 mm ballistic impact specimens.

The construction variables that were included in this investigation were, ply orientation and relative proportions of graphite and S-glass reinforcement fiber. These panels had the following ply orientations.

Type I: $0°, \pm 45°$
Type II: $0°, \pm 22°$
Type III: $0°, \pm 45°, 90°$

The specific dispersed ply construction used for these panels is as follows:

Ply Number	1	2	3	4	5	6	7	8	9	10
Type I	[+45	0	-45	0	+45	0	-45	0	0	0]S
Type II	[+22	0	-22	0	+22	0	-22	0	0	0]S
Type III	[+45	0	-45	90	+45	0	-45	90	0	0]S

The test panels contained three different proportions of graphite and S-glass reinforcing fibers:

Type A: All Graphite
Type B: 80% Graphite, 20% S-Glass
Type C: 60% Graphite, 40% S-Glass

Plies 4 and 7 of the Type B panels (80 graphite/20 glass) and plies 1, 4, 7 and 9 of the Type C (60 graphite/40 glass) were constructed of glass prepreg.

Prior to testing each panel was inspected for density, thickness, and by ultrasonic techniques. All panels were shown to be acceptably uniform and free of flaws by ultrasonic through-transmission inspection. The panel thicknesses and densities were within the acceptable limits.

2. Ballistic Test Results

The test specimens were mounted in a cantilevered fashion in a fixed end support using fiberglass doublers, as shown in Figure 1. The specimens were impacted normal to the major surface with 1.27 cm diameter (1 gm) gelatin spheres at three different velocities in a random sequence within each velocity test group.

Testing was conducted at 275 m/sec, 245 m/sec and 215 m/sec. The velocity of each projectile was measured electronically with photocells immediately prior to impact.

- Visual Observation

The effects of impacts of 215, 245, and 275 m/sec are shown in Figures 2, 3, and 4. A subjective assessment of the nature and relative severity of damage was made. This included characterization of the apparent surface damage at the front and back faces and delamination visible at the specimen edges. General conclusions were:

- The mode of failure for all configurations at the two lower velocities (215 and 245 m/sec) was by moderate cracking or delamination. Ply configuration II ($0 \pm 22°$) was more prone to longitudinal cracking under conditions where the other two ply configurations tended to fail by delamination.

- At the two lower velocities, adding S-glass increased the resistance to crack damage of all ply configurations, but did not reduce delamination damage appreciably.

- Comparing specimens impacted at the two higher velocity levels (245 and 275 m/sec) there did not appear to be a substantial difference in the degree of damage between the different configurations.

- At the higher velocities, while Hybrid B (20 percent S-glass) did not show substantially less damage than 100 percent Modmor II, the inclusion of 40 percent S-glass (Hybrid C) did significantly reduce the severity of damage.

- Ultrasonic C-Scan

Using the initial control ultrasonic through-transmission C-scan as a baseline, impacted panels were measured for continuity. The relative damaged area of each panel was determined through measurement of the area of discontinuity on the C-scan print with a planimeter. Results were averaged for the two panels tested at each condition. The highest value of damaged area was characterized as 100 percent damaged; all others were normalized as a relative proportion of this value.

Figure 5 presents the relative damage in each panel on C-scan. The effect of ply orientation and glass on the C-scan transmission at each velocity level can be summarized as follows:

- Little damage was suffered by any specimens at the lowest velocity, (215 m/sec) indicating that the visual observations of slight cracking essentially defined the limit of damage. Configuration II (0, ±22) was slightly inferior insofar as there was some delamination.

- At the highest velocity (275 m/sec), a high degree of damage was suffered by all configurations. It appears that the highest glass content (40 percent) and Configuration III (0, ±45, 90) were somewhat superior in their respective categories.

- At the intermediate (245 m/sec) velocity, there was a trend for significantly less damage for Configurations I and III as glass content is increased. The results for Configuration II were anomalous.

- At the intermediate velocity the inclusion of 90 degree plies decreased the damage for all compositions, as seen by comparing Configurations I and III.

- At the intermediate velocity, Configuration II shows less damage than the other two. However, the visual observations indicate this may be attributable to the splitting failure mode rather than delamination.

- Flexural Response

Flat panel specimens were subjected to elastic four point flexural loading before and after impacting. The fixture dimensions are shown in Figure 6. Deflection at the center span was recorded for a 115 kg load.

The flexural deflection is an inverse measure of the resistance of the panel to elastic deformation. Low values of reported deflection, therefore, indicate high rigidity or stiffness. It is expectable that the rigidity of untested panels will vary according to their ply configuration and composition. In any given panel, the change in deflection from the baseline is a measure of the impact damage incurred. In most panels, this is a reflection of the change in section modulus (I/c) which can be attributed to delamination. Penetration or fracture of the fibers which prevented load transmission along the length of the specimen was also measured.

The pre-impact stiffness of the flat panels varied according to the glass content and ply configuration as shown in Figure 6. It can be seen that the effect of ply orientation is stronger than glass content as would be expected. Configuration II, the most nearly unidirectional has the highest stiffness. The trend to decreased rigidity with increasing content of glass is approximately the same for all three ply configurations.

Figure 6 also indicates the residual stiffness in panels after 275 m/sec impact. These results compare to the lack of significant change after the 215 m/sec impact and a weaker effect after 245 m/sec impact. It can be seen from Figure 6 that Configuration III is substantially inferior to the other two ply orientations. The effect of glass content is stronger for the configurations which are more susceptible to damage.

Figure 7 is a comparison of the relative damage incurred by the different classes of panels, the strong effect of glass content is again seen. More importantly, a significant difference is observed in the lower relative damage incurred by Configuration I compared to the other two at the higher glass content. On the basis of the flexural data, Configuration I with 40 percent glass content appears the best.

- Microstructure

Selective examination was made of the center cross sectional plane of impacted flat panels to determine trends for change in ply configuration and glass content.

Figure 8 indicates typical internal failures in Type B, 20 percent glass panels. All panels had heavy damage as indicated by the other previously described test methods. Penetration damage and macro- and micro-cracking are pronounced in Configuration I. Configuration II shows

less penetration damage. Although the particular planes examined appear to show less penetration in Configuration III than in I, the former actually had the more severe general damage in visual and flexural evaluations.

Figure 9 indicates somewhat more clearly the trend for glass content in Configuration III. In the specimen with no glass, failure is most severe with penetration and fracture of fibers. Type B, 20 percent glass, showed a reduced degree of penetration, but transverse cracking and delamination still occurred. The substantial improvement noted in Type C, 40 percent glass, is reflected in damage that is largely limited to delamination. There is a good correlation in this group with the other evaluation methods and the microstructural features.

From the microstructural standpoint, although no firm conclusions can be made about ply configuration, it is evident that the inclusion of glass is beneficial in reducing impact effects.

- Summary – Panel Ballistic Testing

Gelatin ball ballistic impacting of flat panels indicated that adding up to 40 percent S-glass to Modmor II PR-286 composites improves resistance to penetration and delamination. This improvement correlated with changes in mechanical properties. The effect of glass content was more marked in some ply configurations. In the dispersed ply flat panels, the character of damage under the same impact event varied with the configuration, ranging from longitudinal splitting, to delamination, to penetration. Based on the relative degree of structural damage determined by the change in panel flexural rigidity, Configuration I (0, ±45 degrees) with 40 percent glass was superior.

D. SIMULATED BLADE SPECIMEN IMPACT STUDIES

The objective of this effort was to determine the effect of fiber composition, ply orientation, projectile mass, section size, leading edge protection and trans-ply reinforcement on the ballistic impact resistance of simulated blade specimens. The specimen selected for this work was double-tapered of constant cross section having a 7.6 cm chord, 20 cm span and an edge thickness of approximately 0.056 cm (Figure 10). This specimen enabled the ballistic testing to be more representative of the actual impacts occurring in turbine engine operation without the expense of fabricating functional airfoils.

1. Fabrication

Standard simulated blades (Figure 10) were fabricated by compression molding 28 plies of prepreg tape for 120 minutes at 138°C. The ply lay-up is shown schematically in Figure 11. The specimens were molded in a die and pressed to stops which resulted in a fiber volume fraction of nominally 0.57 in the finished composite. The lower fiber volume fraction of the starting prepreg material (0.54) permitted a minor amount of resin extrusion to achieve the final value. Panels were then post-cured at 149°C for 16 hours.

Analysis was made to predetermine the specific sequence of ply orientation and material alternation for each of the four ply configurations and three compositions. The designated ply orientation and average composition were readily achieved throughout the constant thickness flat panels. However, the diamond cross section panels had a varying number of ply layers

depending on location from the leading edge. It was difficult to achieve exact consistency with the nominal composition and orientation sequence in the diamond panel, especially in the extreme leading edge where the part consisted of only four plies.

The leading edge to quarter-chord region was considered to be the critical impact resisting region in the ballistic impact testing of similated blade specimens. The layups were selected to achieve the nominal configuration and composition at the quarter chord location. This required variation in the sequence of layup of the different width tape layers.

Specimens thicker than the standard 3.9 mm center line thickness were built up by adding full width plies in a manner consistent with the composition and configuration of the standard specimen, and appropriately increasing the thickness of the die stops during the compression molding. The leading edge in these specimens was increased by an amount equal to the increase of the standard part thickness.

The construction of simulated blades was identical to that of the flat panels insofar as the choice of nominal configuration and composition. One additional configuration was added to the Types I, II and III, [(0°, ±45°), (0°, ±22) and (0, 90, ±45), respectively]. This configuration, designated Type III-A, is similar to Type III, except that the construction is altered so that all 90 degree plies are S-glass in contrast to the Type III specimen in which the 90° plies are a graphite composite material (see Figure 11).

The quality of the simulated blades was evaluated prior to testing. The density, and dimensional uniformity of each simulated blade was measured as was the torsional rigidity of the specimen. The simulated blades were subjected to torsional testing using the fixture shown schematically in Figure 12.

2. Bench Ballistic Testing

Ballistic impact testing was conducted with the setup shown schematically in Figure 13. Impact by a gelatin projectile was on the leading edge. Velocities were pre-calibrated for each projectile mass/velocity combination. As a control, velocities were checked from time to time during the test schedule. During the final stages of the test program, as a result of an improved measuring technique, the velocity was measured for each impact event. Motion picture records were made selectively to ensure that the projectile was intact and properly impacted the specimen.

a. Effect of Ply Orientation and Composition

The aim of ballistic testing of these simulated blade specimens was to determine the effects of ply configuration and glass content and compare these results with those observed in the flat panel ballistic testing. Gelatin projectiles of 2.54 cm diameter (8.5 gm) were used to impact the leading edge of the blade specimen. In all cases the angle between the chord of the blade specimen and the direction of the projectile was 30°. Three projectile velocities were used: 90 m/sec, 150 m/sec and 275 m/sec, to establish an approximate velocity threshold to cause damage. The schematic test plan is shown in Table III.

TABLE III

BALLISTIC TEST PLAN – BLADE SPECIMENS
EFFECT OF PLY CONSTRUCTION AND COMPOSITION

	Type I (0, ±45)	Type II (0, ±22)	Type III (0, ±45, 90)	Type III-A* (0, ±45, 90)
Type A (All Graphite) Velocity (m/sec)				
90	H-2	H-4	H-6	–
150	H-1	H-3	H-5	–
275	H-2	H-4	H-6	–
Type B (80% Graphite) (20% Glass) Velocity (m/sec)				
90	H-8	H-10	H-12	H-14
150	H-7	H-9	H-11	H-13
275	H-8	H-10	H-12	H-14
Type C (60% Graphite) (40% Glass) Velocity (m/sec)				
90	H-16	H-18	H-20	H-22
150	H-15	H-17	H-19	H-21
275	H-16	H-18	H-20	H-22

*90° plies are glass

One specimen of each configuration and composition was impacted at 90 m/sec initially. The damage from this impact was minimal, as shown in Figure 14. The second group of identical simulated blades was impacted at 150 m/sec. Specimens which were hit on one edge during the 90 m/sec test were then hit on the opposing edge at 275 m/sec, and are considered separately here as the third group. In view of the minor damage in the first and lowest velocity impact event, it is not felt that the 275 m/sec results were significantly affected through the double use of the specimen.

Test Results

After testing, simulated blades were subjected to several damage assessments. These included visual, dimensional change, torsional rigidity, and microstructural evaluations.

- Visual Observation

Figures 14, 15 and 16 indicate the condition of the simulated blades after each impact. Visual inspection indicated the following:

- The beneficial effects of glass in raising the damage threshold are seen from the 90 m/sec impact test results. Types B and C suffered little or no damage compared to the all graphite Type A. The presence of 90 degree plies of glass (Configuration III-A) appeared to result in greater damage.

- Similar beneficial results from the inclusion of glass were seen from the 150 m/sec impact test results where the character of the damage was changed from a break out (local loss of material) to fragmentation (fibrous damaged material remains locally). No strong distinction was seen between the 20 and 40 percent glass contents or between the different ply orientations from the 150 m/sec impact testing.

- At the highest velocity, 275 m/sec, all specimens suffered relatively severe damage and qualitative distinctions were difficult. Configuration III seemed inferior, and all graphite specimens suffered the most severe damage.

- At the highest velocity, Configuration II suffered a distinctly different character of damage. This was manifested by fracture and delamination at the corner (tip) opposite the impact edge.

- Dimensional Change

The depth and length of material break out or fragmentation in the impact area was recorded and analyzed. It should be understood that this data is approximate, but may be useful in assessing the effect and need for leading edge protection. Figure 17 shows the data for the depth of break out in specimens tested at 275 m/sec. It can be seen that there is no strong trend with glass content and, that Configurations I and II are better. The effect of 90 degree glass plies is apparently manifested in the superiority of Configuration III-A to Configuration III.

The area of material loss was approximated by calculating the area of a triangle with a base equal to the length of break out. It can be seen from Figure 18 that insofar as configurations are concerned, the trends described for the depth alone are again supported. The most notable difference is that there is a significant increase in damage area as glass content increases. The depth showed no such trend. In these glass containing simulated blades, it appears as though the impact load was distributed more along the length of the specimen.

- Torsional Rigidity

Subsequent to impacting, simulated blades were subjected to torsional testing. Under a steady torsional load of 425 newton-meters, the comparative torsional deflections were measured (or extrapolated for the more severely damaged specimens). Torsional angular deflection is an inverse measure of the structural rigidity. This is a function of the ply configuration and glass content. In simulated blades with these parameters unchanged, torsional rigidity is a measure of the section modulus. Section modulus is affected by delamination, break out and other structural damage. Therefore, change in torsional rigidity is a measure of the damage caused by ballistic impact, although the effect and significance of damage of differing character is a matter of analysis.

Figure 19 indicates the torsional deflections of simulated blades which were impacted at 150 and 275 m/sec. Scheduling problems prevented torsional testing of unimpacted or 90 m/sec impact specimens. However, visual observations of the slightly damaged 150 m/sec specimens and the data in Figure 19 for the 150 m/sec impacted blades indicated that they can serve as an approximate reference point. It can be seen that at 150 m/sec, for the slightly damaged glass containing specimens (Types B and C) there was an expectable trend for increasing deflection (lower rigidity) with glass content increase. The relative rankings of deflections were in accord with the stiffness which would be expected as a result of Configuration differences: II was the least rigid and III-A was the most rigid.

A substantially higher torsional deflection was manifested in specimens after they had been impacted at 275 m/sec. The rankings by configuration were reversed as shown in Figure 19. However, there was little indication of change in deflection for different glass contents. A more meaningful display of this data is made in Figure 20 where the incremental damage is shown. It is evident that Configuration III was greatly inferior to the other two. The substantial decrease in damage in III-A corroborated previous observations for flat panels.

From the results described here, it can be seen that the results in behavior due to impacting of flat panels were similar in trend to those found in simulated blade specimens. Distinctions were found in the specific character and extent of damage due to obvious differences in shape and impact location.

- Microstructure

Several examinations of cross sections of impacted simulated blades were made after torsional testing to determine trends with glass content. These examinations showed that with all-graphite specimens, a clean break out of material occurs at the impact area. With Type B and C specimens, ply separations and fragmentation were pronounced indicating a greater transfer of the impact load into the specimen.

- Summary

The ballistic test data indicated that both the Type I (0, ±45) and the Type II (0, ±22) orientations are superior in resisting impact damage to the Type III (0, ±45, 90) orientation. Quantitative assessment of the degree of damage indicated little difference between the Type I and

Type II orientation. The Type II specimen suffered trailing edge tip splitting upon ballistic impact – a failure mode unique to this construction. It does not seem likely that this type of failure can be prevented by the incorporation of a leading edge protection scheme.

The gelatin projectile impacts caused a break out of a relatively small area in the all-graphite specimens while the specimens containing glass reinforcement had larger damage zones attributable to absorption of projectile momentum by the target blade. The addition of a protective leading edge would preclude the punch-out damage seen in the all-graphite specimen. An effective leading edge would also tend to distribute the impact load more uniformly through the blade and thus the impact performance of the protected blade would be similar to the flat panel studies. These flat panels studies indicated significant improvement with the 40 percent glass fiber reinforcement at the higher velocities.

Based on these results, the Type I (0, ±45) configuration with a Type C hybrid (60% graphite – 40% glass) composites was chosen for the remainder of the effort.

b. Effect of Projectile Mass and Blade Specimen Thickness

Based on the previous results Configuration IC (0° ±45°) 60% graphite/40% S-glass, specimens were chosen to study the effect of projectile mass and blade thickness. The blade specimen length and chord were maintained and full chord width plies were added to increase the blade specimen thickness. Four specimen thicknesses were tested: 3.9 mm (standard); 4.4 mm, 5.4 mm, and 7.4 mm; these specimens had leading edge thicknesses of 0.5 mm, 1.0 mm, 2.0 mm, and 4.0 mm, respectively. Three sizes of gelatin projectiles, 1.27 cm. 2.54 cm, and 5.08 cm, were used. The projectiles were accelerated to nominally 275 m/sec prior to impact at a 30° angle to the blade chord. The 5.08 cm projectiles were accelerated to 245 m/sec. Specimen mounting and ballistic testing technique were identical to those described previously.

- Test Results and Discussion

Visual examination of the tested specimens revealed an increase in ballistic damage resistance with increasing specimen thickness. When impacted with the 1.27 cm diameter gelatin projectile, the standard thickness blade specimen (3.9 mm) suffered damage to the leading edge. The next thicker specimen (4.4 mm) incurred very slight damage. The 2.54 cm diameter gelatin projectile caused extensive damage to both the standard (3.9 mm) and the 4.4 mm thick blade specimen but only minor damage to the 5.4 mm thick specimen. Finally, the 5.08 cm diameter projectile caused complete loss of structural integrity of the 5.4 mm thick specimen and some delamination damage to the 7.4 mm thick specimen. These specimens after impact are shown in Figure 21.

The torsional deflection of the blade specimens under a constant load before and after impact was measured as described earlier in the report. Since torsional deflection varied with the thickness of the specimen and since loss of rigidity of the blade is the more meaningful parameter, the results of the torsional testing are plotted in terms of the normalized loss of rigidity $(1/\theta_i - 1/\theta_f) / (1/\theta_i)$, vs. blade thickness. θ_i is the angular deflection measured for the

blade specimen prior to ballistic impact testing and θ_f is the angular deflection measured after impact testing.

The results of the torsional testing are shown in Figure 22. The testing of three different thicknesses of blade specimen with 2.54 cm diameter gelatin projectiles resulted in an excellent correlation with loss of torsional stiffness. The test results from the 1.27 cm diameter gelatin projectile impacts plotted parallel to the 2.54 cm diameter plot (Figure 22). These test results provided a degree of confidence in the use of the loss of torsional rigidity as a quantitative measure of ballistic damage. The damage caused by 5.08 cm diameter gelatin projectiles (at a slightly lower velocity) is represented by two data points. Since one of the points is representative of the total loss of specimen rigidity, the relationship between the loss of torsion rigidity and specimen thickness was approximated by drawing a line parallel to the 1.27 cm and 2.54 cm diameter projectile lines through the data point where less than total destruction of the specimen occurred.

Extrapolating the plots of loss of torsional rigidity vs. blade thickness (Figure 22) zero loss of torsional rigidity results in a blade leading edge thickness of 0.11 cm to withstand a 1.27 cm diameter gelatin projectile impact; of 0.20 cm to withstand a 2.54 cm diameter gelatin projectile impact; and of 0.58 cm to withstand a 5.08 cm gelatin projectile impact under the given test condition. The first two points were well supported by the test data while the blade thickness to resist the 5.08 cm diameter gelatin projectile impact is based on a single data point.

To attempt to generalize the results from these tests to the ability of composite fan blades to withstand the ingestion of foreign objects, a plot of minimum blade thickness for zero loss of torsional rigidity (from Figure 22) vs. the normal component of projectile momentum was made (Figure 23). Selection of the normal component of projectile momentum as a parameter allows the inclusion of the angle of projectile incidence to the blade chord, the mass of the projectile and the projectile velocity. At least a qualitative rationale for this parameter was developed in previous work on FOD (Reference 1).

Two points are plotted in Figure 23 from the testing of JT9D fan blades (Reference 2). The point shown for the starling impact which caused very little blade damage lies close to the "no damage" zone of the plot while the second point representing impact by a 8.4 cm gelatin projectile which caused severe blade damage lies well in the "damage" zone of the plot.

Emphasizing that this plot (Figure 23) is based on very little data and requires verification, particularly at higher values of momentum, it does provide an indication that significant protection must be achieved from metallic leading edges to permit the application of composite material blades to withstand 1000 gm birds at current blade thickness designs.

c. Effect of Leading Edge Protection

To establish the capability of the hybrid composite blade construction with a metallic leading edge in ballistic FOD testing, blade specimens were fabricated using all-graphite and graphite and glass hybrid (Type 1A and 1C). In addition Ti-6Al-4V alloy material in identical geometry to the composite specimens was used.

The construction of the composite blade specimens with metal leading edge protection is indicated in Figure 24. AISI 322 stainless steel sheet 0.25 mm thick was wrapped around and spot welded at close intervals along the AISI 304 leading edge insert. This metal assembly was then bonded to the composite blade with Miller Stephenson 907 epoxy adhesive using the steel die normally used in panel construction. Conventional cleaning techniques were used for preparing the composite and stainless steel surfaces prior to bonding. Visual inspection and end-sectioning indicated that a satisfactory fit and bond were achieved.

Bench ballistic impact testing was conducted using 15 blade specimens. These specimens included the all-graphite, 0, ±45° (Type 1A) with and without leading edge protection, the hybrid 40% glass, 0, ±45° (Type 1C) with and without leading edge protection and titanium alloy (Ti-6Al-4V) specimens. Gelatin projectiles 1.27 cm, 2.54 cm and 5.08 cm in diameter were accelerated to 275 m/sec (245 cm/sec for the 5.08 cm diameter projectile) and impacted the specimens at a 30° angle to the blade chord.

- Test Results

Visual examination of the impact tested specimens (Figure 25) indicated that for the 1.27 cm and 2.54 cm diameter gelatin projectile impacts, the leading edge protection afforded protection to both the all-graphite and the hybrid composite blade specimens. The extent of damage was comparable to that incurred by the titanium alloy blade specimen. The metal leading edge remained completely bonded to the composite material in all cases.

Impacting with the 5.08 cm (66 gm) gelatin projectile resulted in severe damage to all specimens including the titanium alloy blade specimen. The leading edge shields became separated from the composite specimen. The hybrid composite specimen exhibited less damage than the all-graphite specimen indicating some improvement in impact performance through the incorporation of the fiberglass material.

The torsional testing of the blade specimens with the metal leading edge did not provide a quantitative assessment of damage.

The damage caused to the titanium alloy blade specimen by the 5.08 cm diameter gelatin projectile was more severe than engine experience would predict. The presence of part span shrouds which tend to permit the titanium blades to act as a unit rather than individually in resisting impact damage probably is a major contributory factor in the ability of titanium blades to resist impact damage.

d. Effect of Trans Ply Reinforcement

To assess alternate schemes for improving the resistance to ballistic impact damage, a series of blade specimens was constructed. These specimens included the incorporation of trans ply reinforcement (metal staples) to reduce the tendency to delaminate and specimens with "Kevlar" organic fiber replacing the fiberglass reinforcement. Specimen construction was 0°, ±45° ply orientation with 60% graphite (Type 1C) as has been described previously. Blade specimen No. H 50, 51, 52, and 55 included metal trans ply reinforcement extending from the leading edge to approximately one quarter chord. This reinforcement consisted of metal

staples made of 0.64 x 1.27 min rectangular wire with 9.5 mm bridge length. To anchor the staples one surface ply of graphite was replaced with one layer of 200 mesh stainless steel screen. The staples were inserted into the laid-up preform prior to molding the blade specimens. (To insure comparative ballistic test results, one specimen, H 49, was fabricated without trans ply reinforcement, but with the metallic screen addition).

Previous ballistic tests with 5.08 cm gelatin projectiles at 245 m/sec at a 30° impingement angle to the blade chord had resulted in destruction of the specimen. Therefore, the ballistic testing of trans ply reinforcement specimens included tests at a 15° angle to the blade chord, including a control specimen without the trans ply reinforcement.

The test schedule is summarized as follows:

CONSTRUCTION AND TEST CONDITIONS OF
TRANS PLY REINFORCED BLADE SPECIMENS

BLADE NUMBER	STAPLES	LEADING EDGE	PROJECTILE DIAMETER (CM)	VELOCITY (M/SEC)	ANGLE (°)
H-49	–	–	2.54	275	30
H-50	X	–	2.54	275	30
H-51	X	X	5.08	245	30
H-52	X	X	5.08	245	15
H-53	–	X	5.08	245	15
H-54[1]	–	–	2.54	275	30
H55[1]	X	–	2.54	275	30

1 – S-Glass replaced with "Kevlar"

- Test Results

The effect of replacing the S-glass in a standard Configuration I Type C specimen (H 16) with Kevlar was evaluated (H 54). The "Kevlar" specimen was locally fragmented at the point of impact. Delamination was confined to the area of impact. Surface ply loss was found on the back of the specimen between the point of impact and the trailing edge. The normalized loss of torsional rigidity was 41%. In comparison, specimen H 16 impacted at the same conditions was found to be fragmented at the point of impact and extensively delaminated. The normalized loss in torsional rigidity was 56%, thus indicating improvement with "Kevlar".

The effect of trans ply reinforcement on the ballistic impact resistance of the standard Configuration I Type C specimen was determined (H 50). This specimen was locally fragmented at the point of impact. Minor delamination was confined to the area of impact and did not extend beyond one third of the chord length from the impact. The normalized loss in torsional rigidity was 22%. In comparison the unreinforced standard specimen (H 16) impacted at the same conditions was fragmented at the point of impact and extensively delaminated. Trans ply reinforcement significantly increased the resistance to delamination of this type of specimen.

The effect of trans ply reinforcement on the impact resistance of the "Kevlar" modified standard Configuration I Type C specimen was evaluated. The reinforced specimen (H 55) suffered local fragmentation at the point of impact with most of the fragments retained by trans ply reinforcements. Minor localized delamination was associated with the impact area. A 22% loss in torsional rigidity was measured.

The reinforced Kevlar modified specimen (H 54) was locally fragmented at the point of impact. Delamination was confined to the area of impact but was more extensive than in the reinforced specimens. Surface ply loss was found on the back of the specimen between the point of impact and the trailing edge. A 41% loss in torsional rigidity was measured. When compared to the trans ply reinforced standard Graphite/S-Glass specimen (H 50) the reinforced Kevlar specimen (H 55) suffered similar damage with the same loss in torsional rigidity. Trans ply reinforcement improves the ballistic impact resistance of Kevlar modified specimens but does not give performance superior to trans ply reinforced standard Graphite/S-Glass specimens. The impacted blade specimens are shown in Figure 26.

The effect on ballistic impact resistance of the stainless steel surface plies used to anchor the trans ply reinforcements was also evaluated. Specimen H 49 which had surface anchor plies suffered fragmentation near the point of impact. Moderate delamination occurred which extended through 3/4 of the specimen. A 37% loss in torsional rigidity was measured. The damage was similar to the standard specimen (H 16) but slightly less extensive as indicated also by the loss in torsional rigidity. The surface anchor ply appears to improve impact resistance but to a lesser degree than the trans ply reinforcement.

The loss of torsional rigidity of the various configurations is summarized in Figure 27.

The ability of reinforced and nonreinforced specimens with leading edge protection to resist 5.08 cm diameter gelatin ball impacts at 30° to the blade chord and nominally 245 m/sec velocity was studied. The specimens were Configuration I Type C and of standard thickness. Specimen H 51 was extensively delaminated. In the vicinity of the trans ply reinforcement there appeared to be little damage, but several delamination planes were observed forward of that location extending the length of the simulated blade. The rear side of the specimens also suffered delamination which extended along the length and from the trans ply reinforcement location to the trailing edge. The stainless steel leading edge protector was separated and extensively deformed during the impact. Adherence of surface plies to the separated leading edge indicated adequate bond to the specimen.

A second specimen identical to H 51 was impacted at the same conditions except for the angle of impact. It was impacted at 15° to the leading edge to reduce the damage and thereby permit a more realistic comparison to the unreinforced control specimen. Specimen H 52 suffered minor localized delamination behind the trans ply reinforcement in the vicinity of the impact. The leading edge protector was distorted in the area of the impact but remained bonded to the specimen along most of its length. A bending type structural failure was incurred near the specimen support. Minor delamination was associated with the fracture near the trailing edge. A control specimen identical to the previous two but without trans ply reinforcement was also impacted at 15° to the leading edge with a 5.08 cm diameter gelatin ball at nominally

245 m/sec. Specimen H 53 showed minor delamination and localized loss of surface plies behind the leading edge protector in the vicinity of impact. Bond between the specimen and the leading edge protector was maintained along most of the specimen length. These specimens after impact testing are shown in Figure 28.

The improvement in ballistic impact resistance, if any, afforded by trans ply reinforcement of leading edge protected specimens is unclear. The extent of delamination appears to be reduced by the reinforcement, but the reinforced specimen is apparently more prone to bending structural failure.

3. Spin Impacting of Simulated Blades

Spin impact testing was conducted to determine the effect of applied stress on the performance of blade specimens under impact conditions. The testing was conducted at Hamilton Standard Division of United Aircraft. Rotating simulated blade specimens were impacted at mid-span under conditions described as follows:

TEST CONDITION	SPECIMEN TYPE		
30° TO L.E.	HYBRID WITHOUT L.E.	HYBRID WITH METAL L.E.	TITANIUM
2.54 cm dia. Gelatin at 275 m/sec	X	X	X
5.08 cm dia. Gelatin at 275 m/sec	X	X	X
2.54 cm dia. Gelatin at 400 m/sec	X	X	X

The hybrid construction, Type IC, and leading edge schemes used were the same as that selected for the leading edge protection tests described previously in this report.

Test Results

The spin impact tests using the 2.54 cm gelatin projectiles resulted in damage to the leading edge of the unprotected specimen with only minor denting of the leading edge of the protected composite specimen and the titanium alloy reference specimen (Figure 29).

Using the 5.08 cm gelatin projectile severe damage was inflicted upon the unprotected specimen while debonding of the protective sheath and some blade damage was evident on the protected composite blade. The titanium specimen exhibited minor denting of the leading edge (Figure 29).

Using the 2.54 cm gelatin projectiles and spinning the blades at the higher velocity of 400 m/sec resulted in moderate damage to the unprotected specimens. The leading edge sheath protected the composite blade during impact although denting of the leading edge and some debonding of the sheath were evident. The titanium specimen suffered minor denting during impact at the high velocity conditions (Figure 29).

Torsion testing of the unprotected specimens indicated little loss in torsional rigidity following the 2.54 cm gelatin projectile impact at 275 m/sec, substantial loss in rigidity after the 2.54 cm gelatin projectile impact at 400 m/sec and the destruction of the blade when impacted by the 5.08 cm gelatin projectile at 275 m/sec prevented measurement of post-test torsional rigidity.

The presence of the metallic leading edge prevented meaningful quantitative damage assessment by the measurement of torsional rigidity.

The spin impact testing resulted in less damage to the specimens than the bench testing. Since high speed motion pictures were not taken of the spin impact tests it is not clear whether the "slice size" was less than intended, thus resulting in a less severe impact, or whether the spin test is less severe than the bench test.

IV. CONCLUSIONS

The following conclusions are drawn from this study.

- The inclusion of fiberglass or "Kevlar" reinforcement improves the ballistic impact resistance of graphite composite material although not to the extent indicated by Charpy impact values.

- The addition of trans ply metallic reinforcement improves the ballistic impact resistance of graphite fiber composite blades.

- Metallic leading edge protection permitted composite blades to survive 2.54 cm diameter gelatin projectile impacts but was not successful in protecting against 5.08 cm diameter gelatin projectiles.

- Bench ballistic testing of titanium blade specimens was more severe than engine experience.

REFERENCES

1. Friedrich, L. A. and Preston, J. L. Jr., "Impact Resistance of Fiber Composite Blades Used in Aircraft Turbine Engines, NASA CR-134502, May 1973.

2. Premont, E. J. and Stubenrauch, K. R., "Impact Resistance of Composite Fan Blades", NASA CR-134515, May 1973.

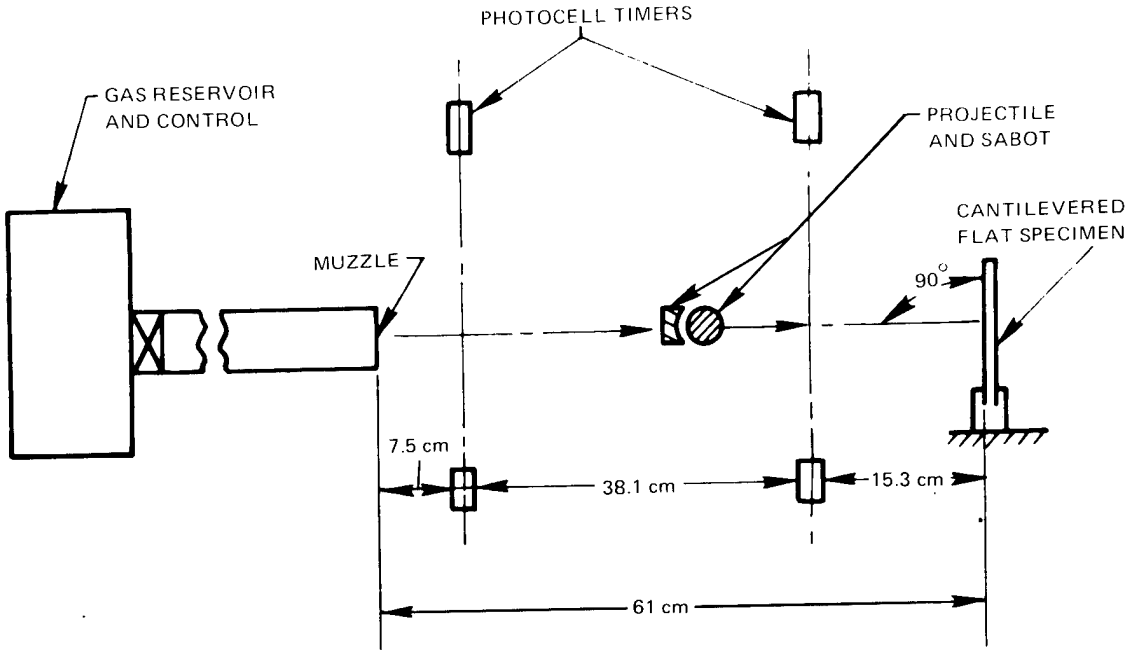

(a) ANGLE AND DISTANCE

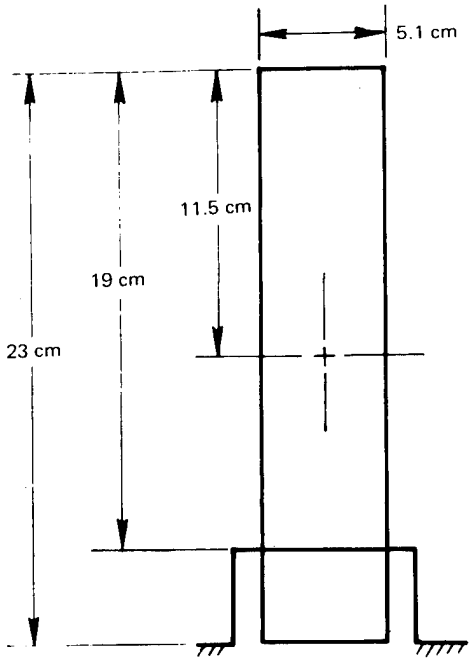

(b) HOLDER

Figure 1 Schematic of Ballistic Impact Test for Flat Panels

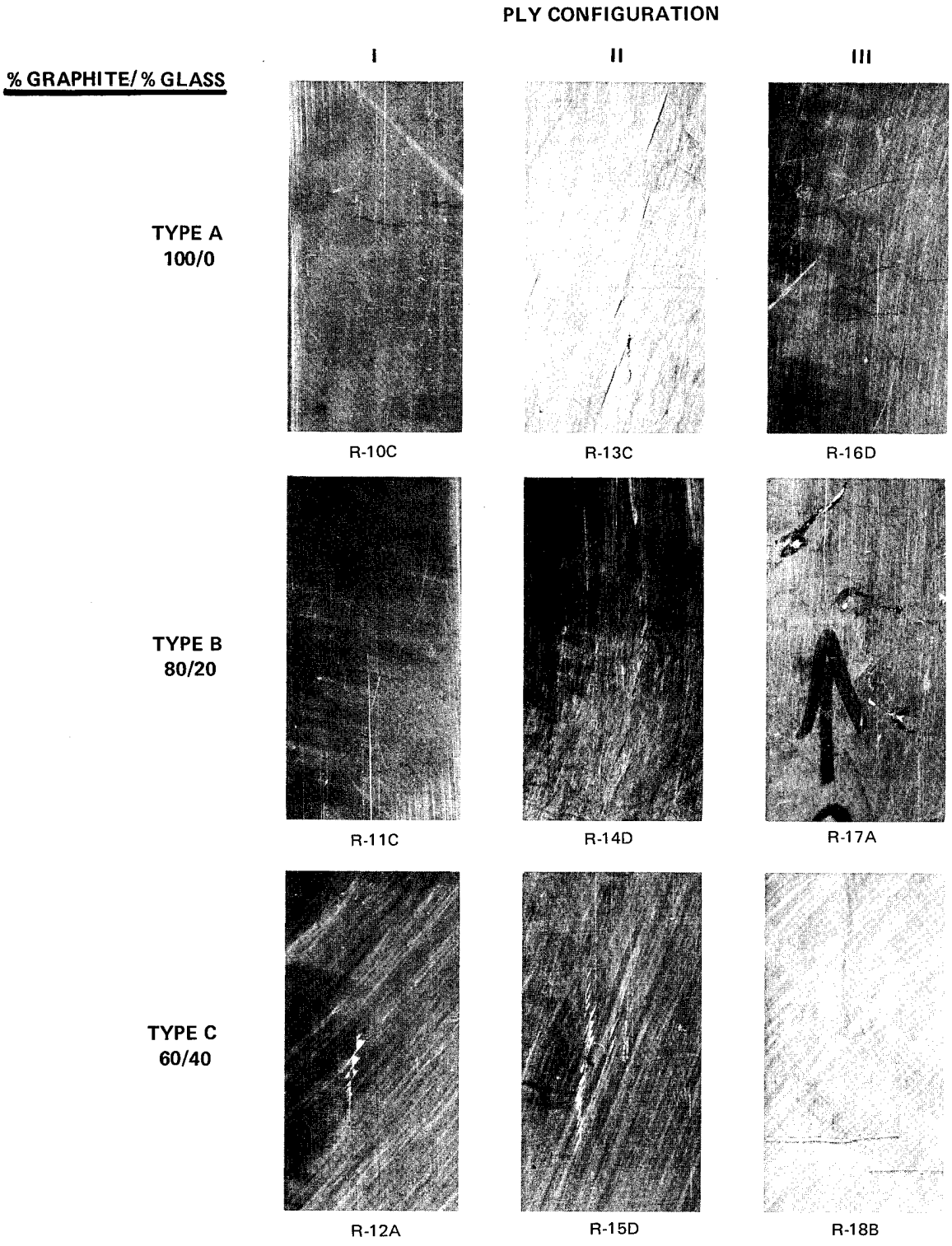

Figure 2 Damage to the Back Face of 5 x 23 cm Flat Panels When Impacted with 1.27 cm Diameter Gelatin Balls at a Velocity of 215 m/sec

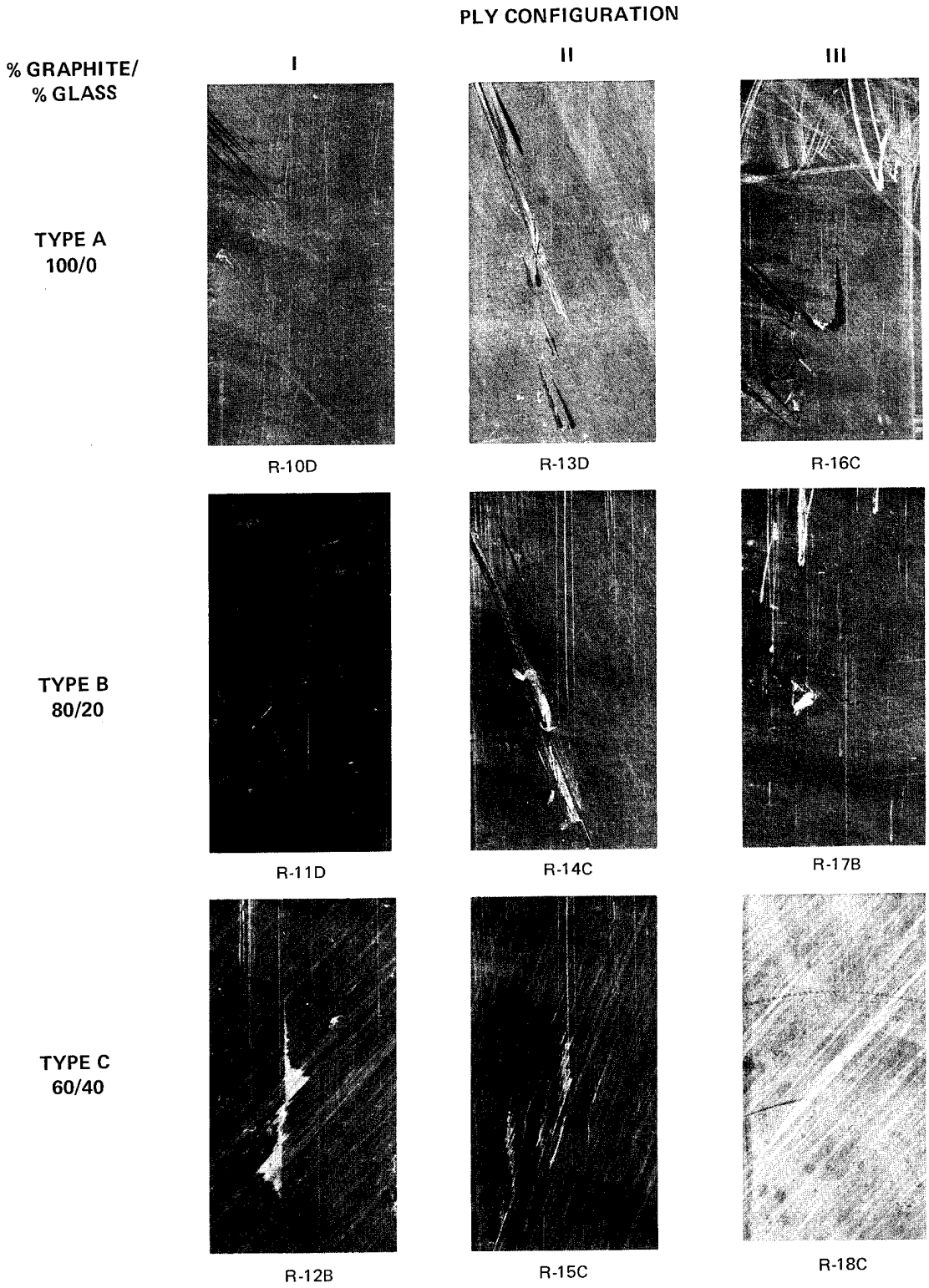

Figure 3 Damage to the Back Face of 5 x 23 cm Flat Panels When Impacted with 1.27 cm Diameter Gelatin Balls at a Velocity of 245 m/sec

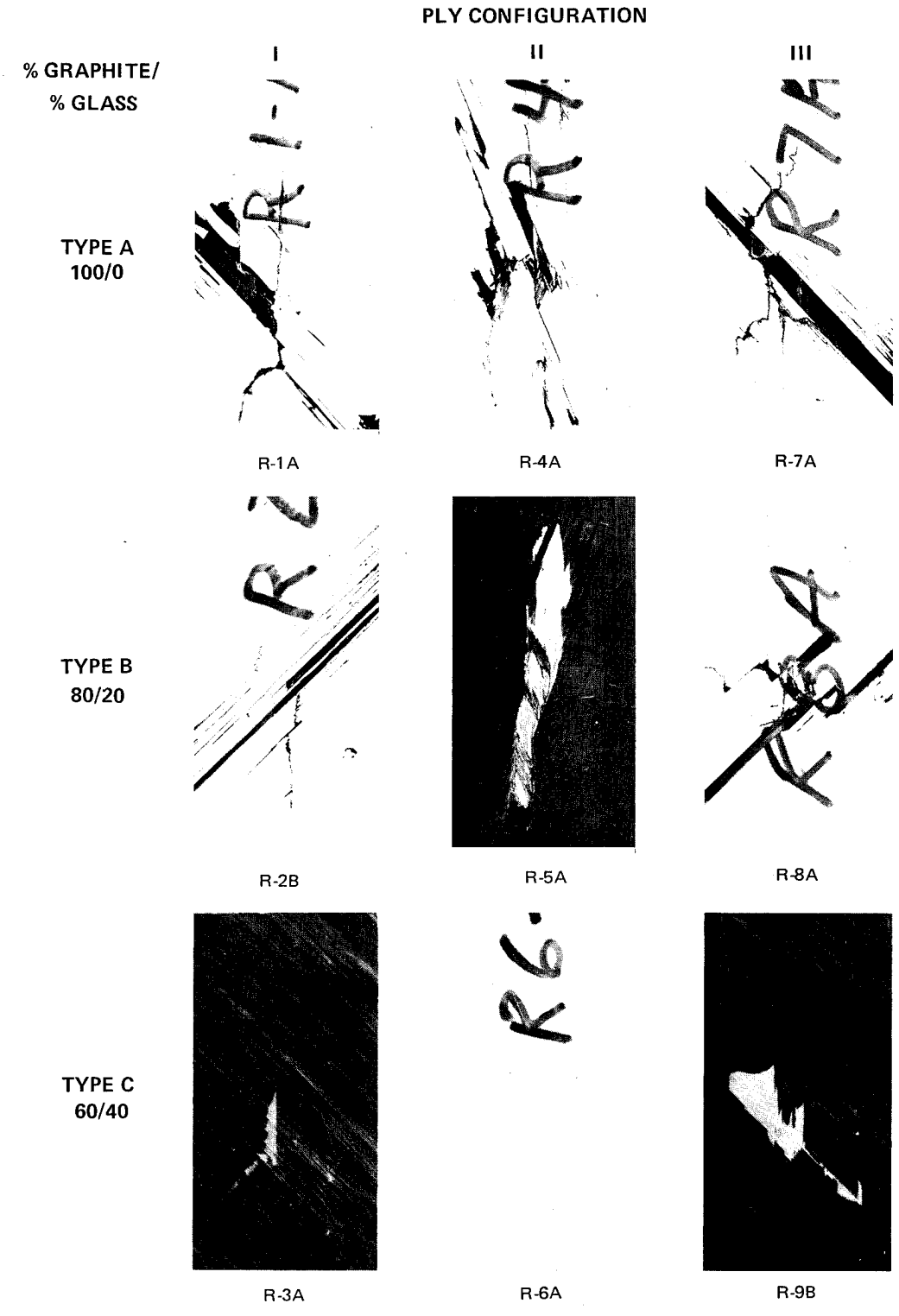

Figure 4 Damage to the Back Face of 5 x 23 cm Flat Panels When Impacted with 1.27 cm Diameter Gelatin Balls at a Velocity of 275 m/sec

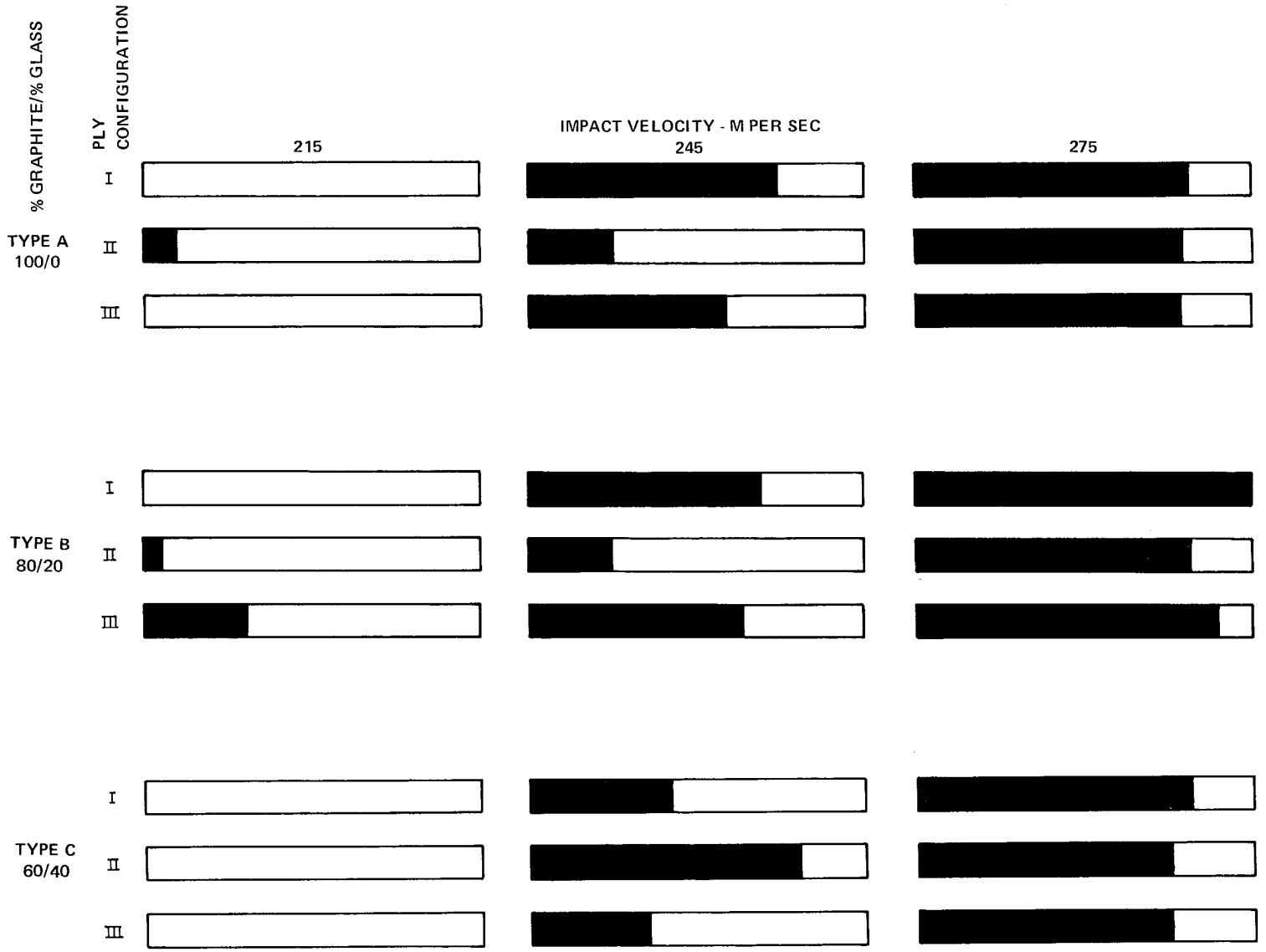

Figure 5 Relative Damage as Determined by Ultrasonic C-Scan in 23 x 5 cm Flat Panels After Ballistic Impact with a 1.27 cm (1 gm) Gelatin Ball at 275 m/sec. Damage was Normalized by Assigning the Most Damaged Specimen a Value of 100 and Determining the Relative Damage of All Others

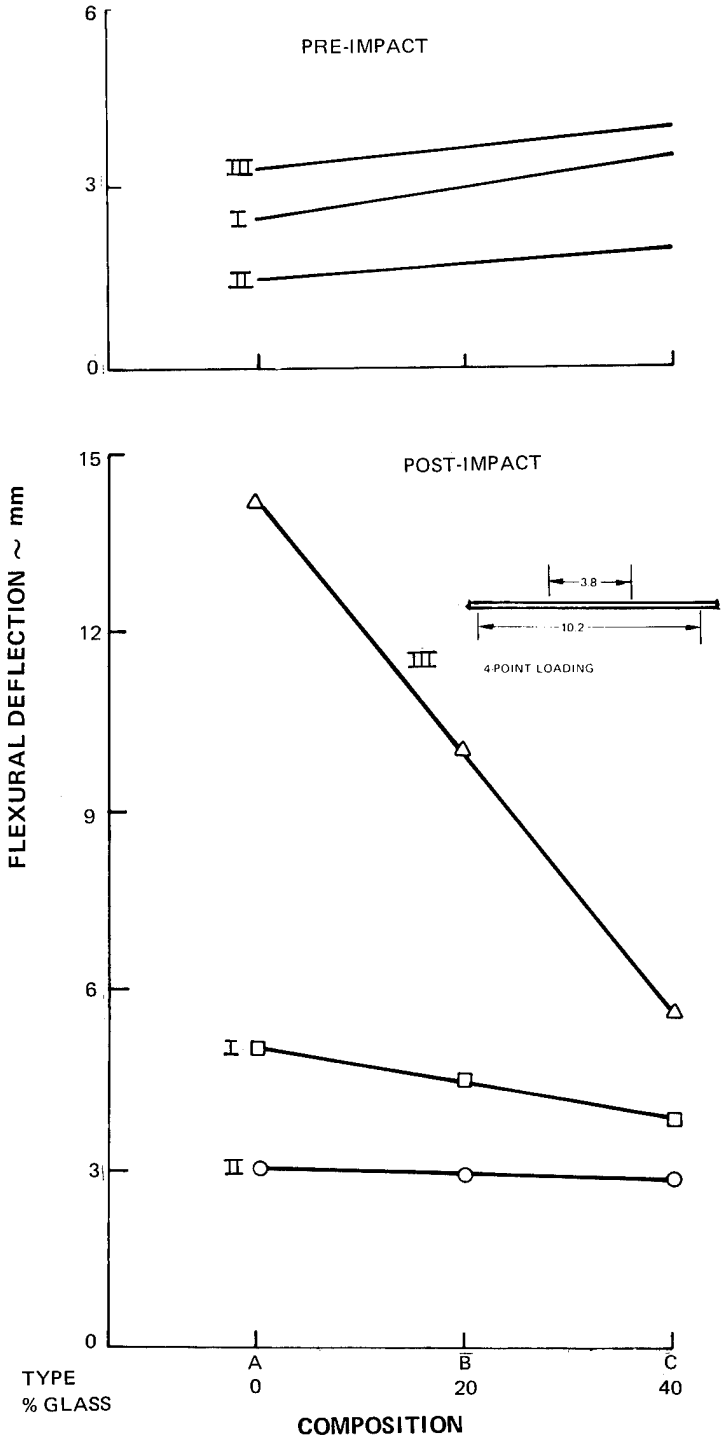

Figure 6 Stiffness of Flat Panels Before and After 275 m/sec Ballistic Impact. Pre-Impact Rigidities Largely Reflect Ply Orientation. Post-Impact Stiffness is Retained Best By Higher Glass Content Specimens and Configurations I and II

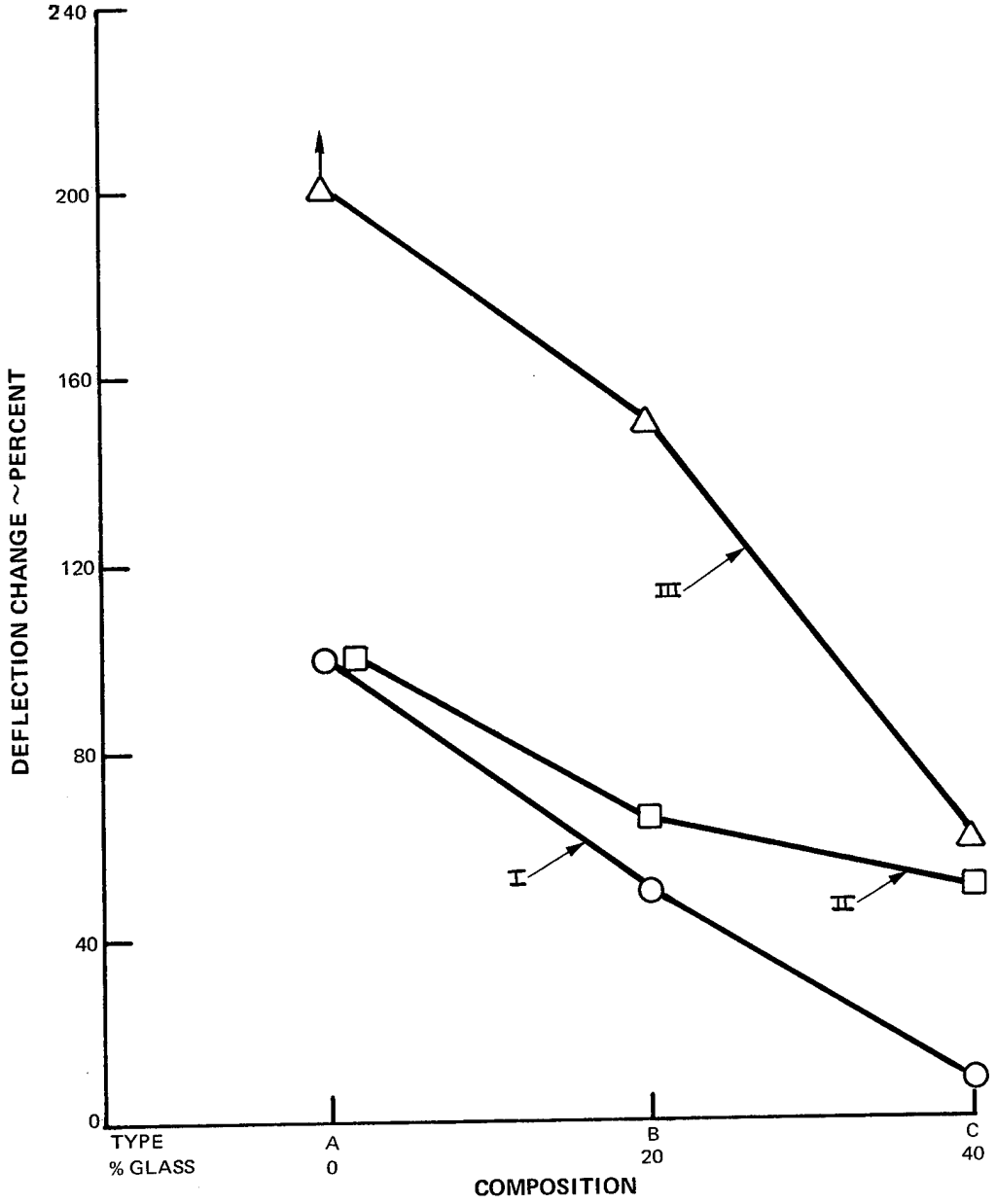

Figure 7 Relative Damage in Flat Panels Due to 275 m/sec Impact as a Proportion of Original Flexural Rigidity is Sharply Decreased by Inclusion of Glass. Configuration I Appears Superior

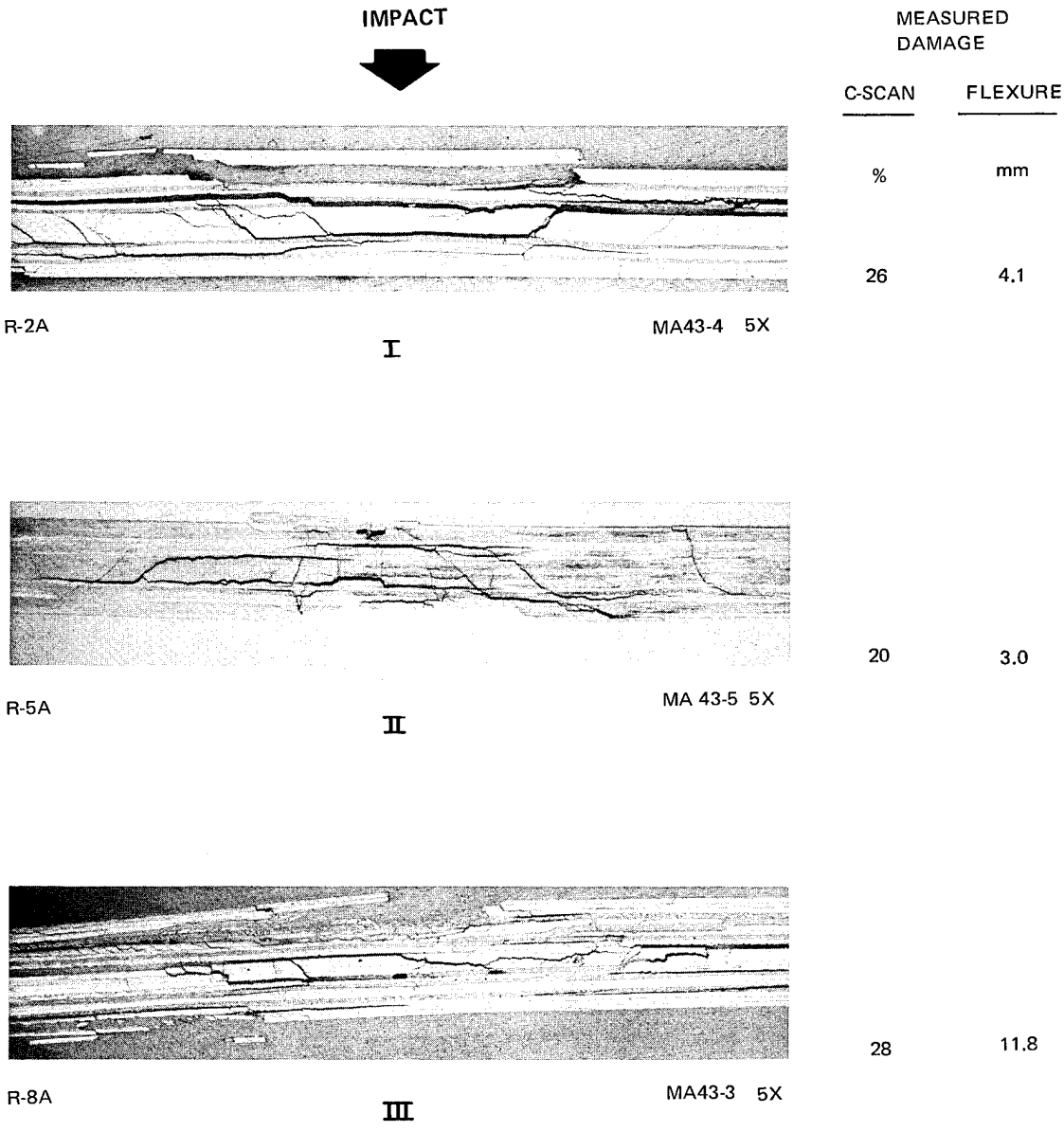

Figure 8 Microstructural Damage in Type B (20% Glass) Flat Panel Center Cross Sectional Plane After 275 m/sec Impact

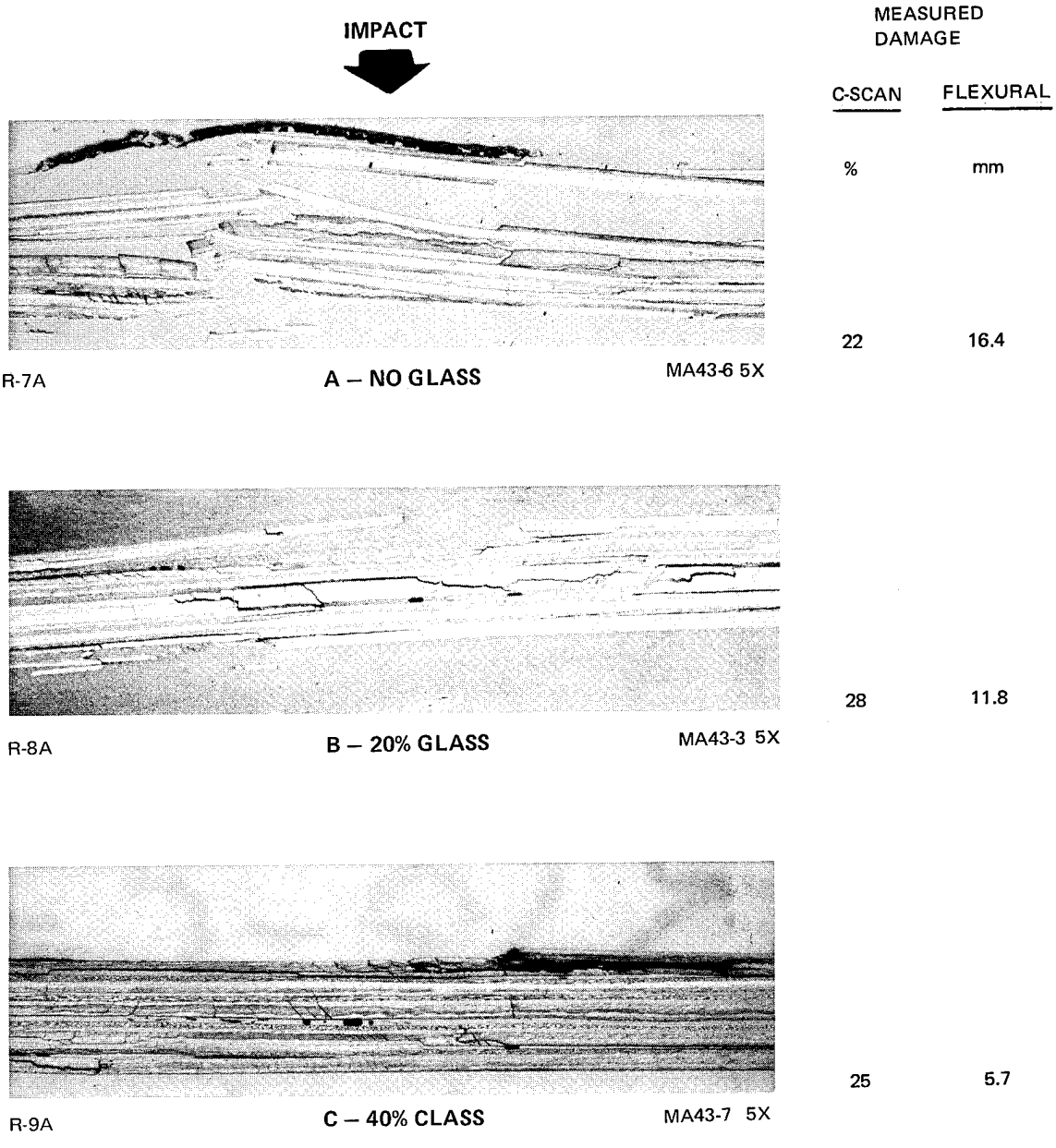

Figure 9 Microstructural Damage in Configuration III Flat Panel Center Cross Sectional Plane After 275 m/sec Impact. Less Severe Damage is Evident in Higher Glass Content Panels

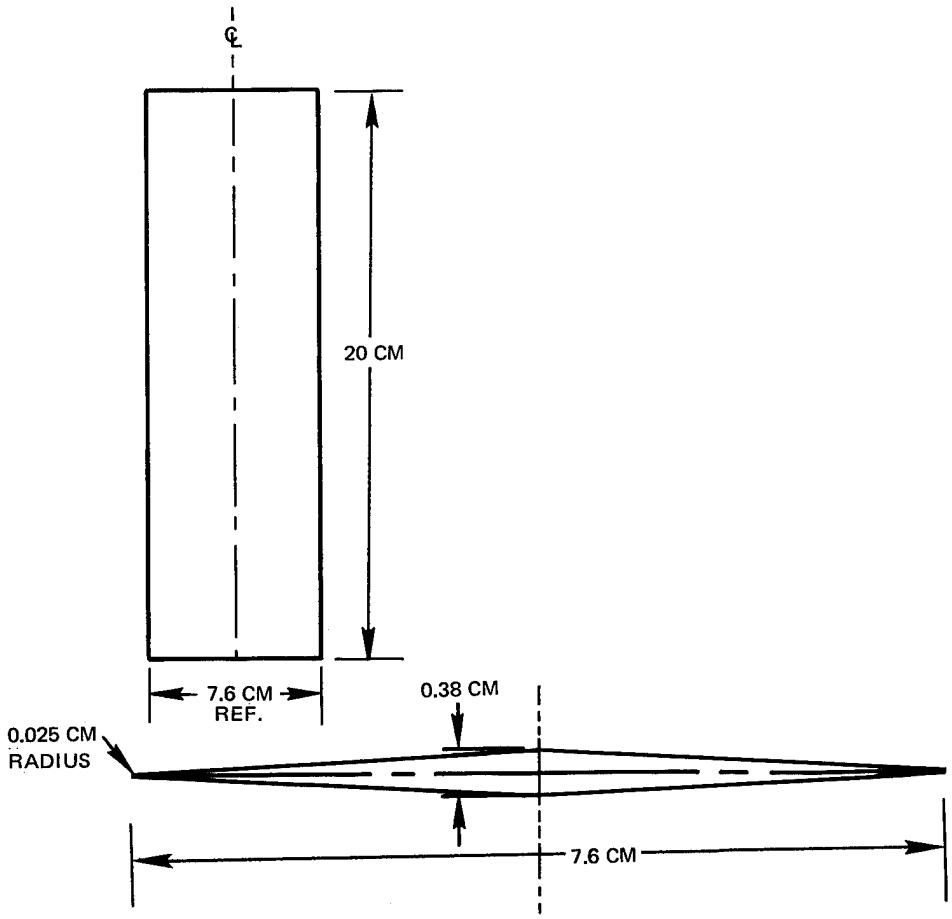

Figure 10 Simulated Blade Impact Specimen

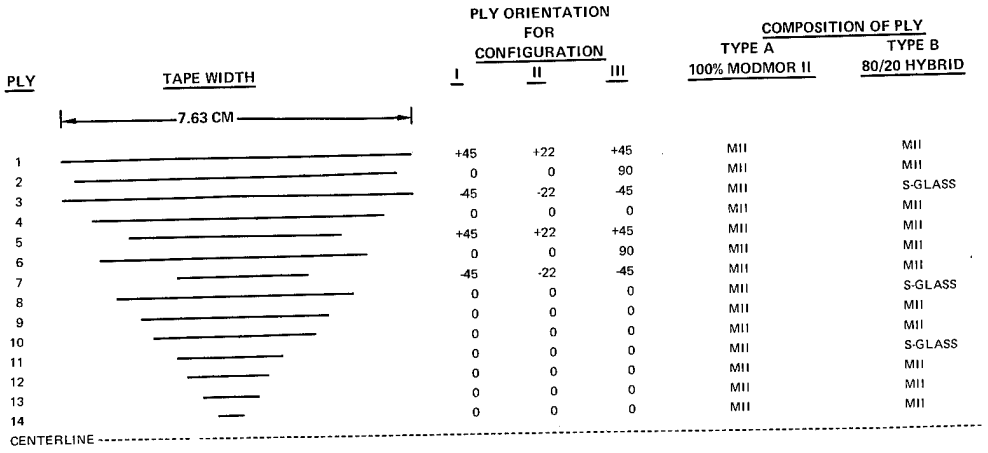

PLY	PLY ORIENTATION FOR CONFIGURATION I	II	III	COMPOSITION OF PLY TYPE A 100% MODMOR II	TYPE B 80/20 HYBRID
1	+45	+22	+45	MII	MII
2	0	0	90	MII	MII
3	-45	-22	-45	MII	S-GLASS
4	0	0	0	MII	MII
5	+45	+22	+45	MII	MII
6	0	0	90	MII	MII
7	-45	-22	-45	MII	MII
8	0	0	0	MII	S-GLASS
9	0	0	0	MII	MII
10	0	0	0	MII	MII
11	0	0	0	MII	S-GLASS
12	0	0	0	MII	MII
13	0	0	0	MII	MII
14	0	0	0	MII	MII

a) Type A and B Composites

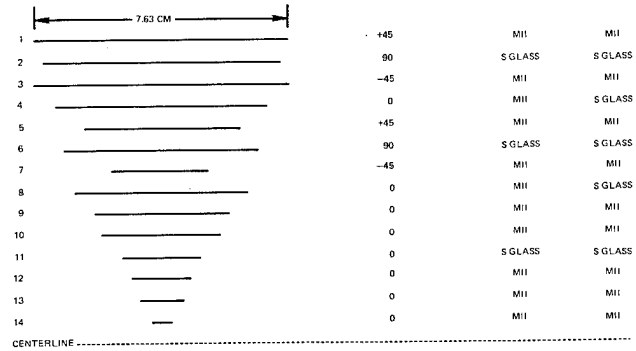

PLY	PLY ORIENTATION FOR CONFIGURATION III-A	COMPOSITION OF PLY TYPE B 80/20 HYBRID	TYPE C 60/40 HYBRID
1	+45	MII	MII
2	90	S GLASS	S GLASS
3	−45	MII	MII
4	0	MII	S GLASS
5	+45	MII	MII
6	90	S GLASS	S GLASS
7	−45	MII	MII
8	0	MII	S GLASS
9	0	MII	MII
10	0	MII	MII
11	0	S GLASS	S GLASS
12	0	MII	MII
13	0	MII	MII
14	0	MII	MII

b) Type B and C Composites Made in Configuration III-A Which Utilizes S-Glass for 90 Percent Reinforcement

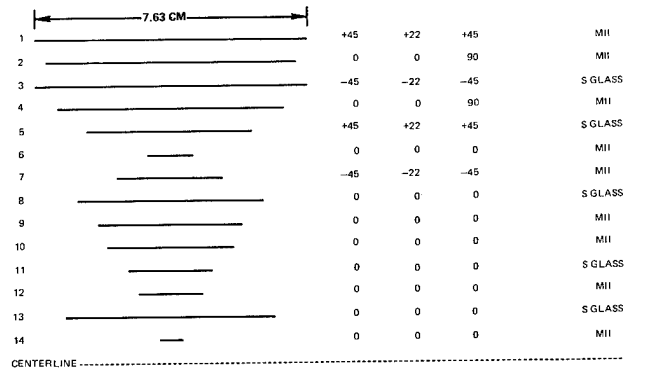

PLY	PLY ORIENTATION FOR CONFIGURATIONS I	II	III	COMPOSITION OF PLY TYPE C 60/40 HYBRID
1	+45	+22	+45	MII
2	0	0	90	MII
3	−45	−22	−45	S GLASS
4	0	0	90	MII
5	+45	+22	+45	S GLASS
6	0	0	0	MII
7	−45	−22	−45	MII
8	0	0	0	S GLASS
9	0	0	0	MII
10	0	0	0	MII
11	0	0	0	S GLASS
12	0	0	0	MII
13	0	0	0	S GLASS
14	0	0	0	MII

c) Type C Composites

Figure 11 Construction of Blade Specimens Showing Layup for Hybrid Composites. Also Shown is the Relative Location and Relative Width of Graphite and Glass Layers

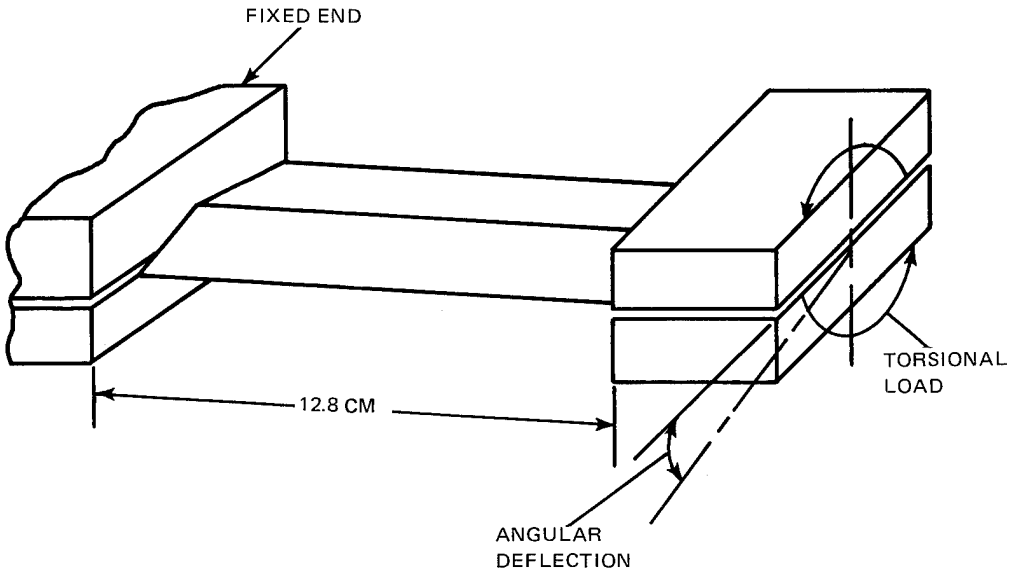

Figure 12 Schematic of Fixture for Torsional Load Testing of Blades

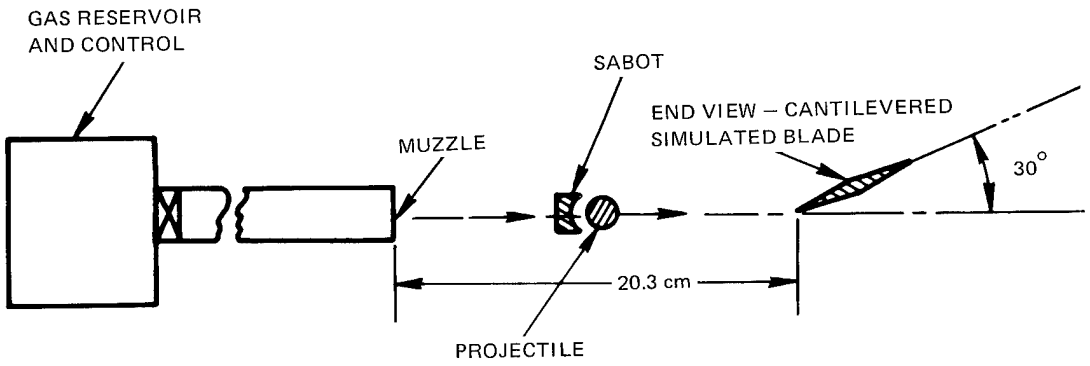

(a) ANGLE AND DISTANCE FROM MUZZLE

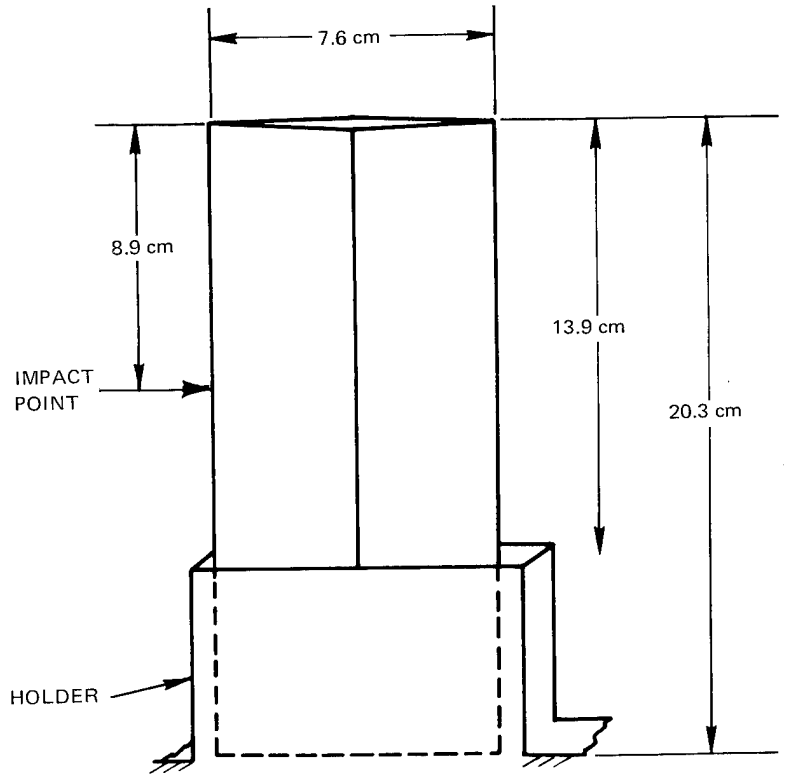

(b) HOLDER AND IMPACT LOCATION

Figure 13 Schematic of Ballistic Test for Blade Specimens

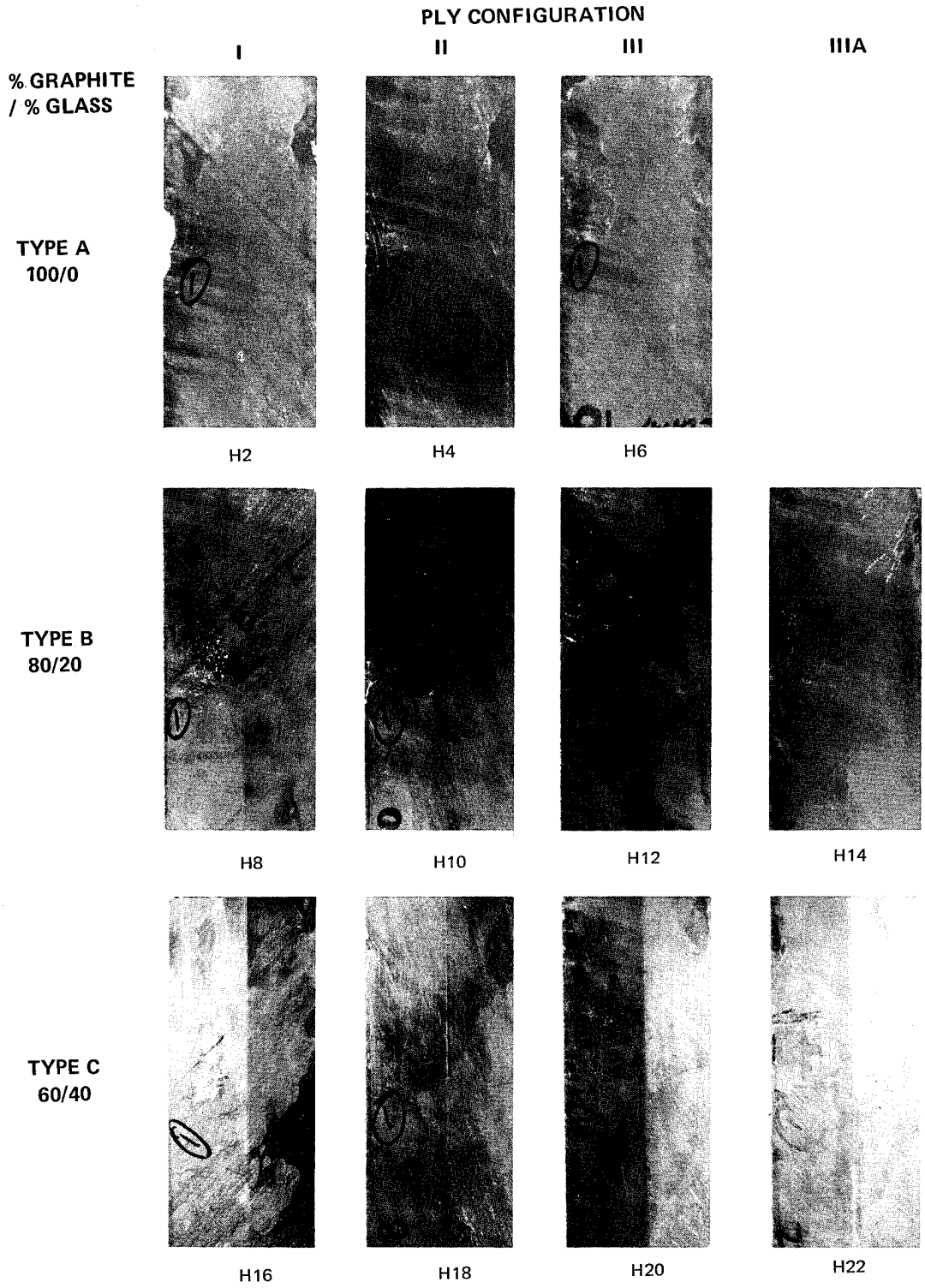

Figure 14 Impacted Composite Blades Showing Damage to the Impact Face From a 2.54 cm Diameter (8.5 gm) Gelatin Ball at a Velocity of 90 m/sec and 30° to the Blade Chord

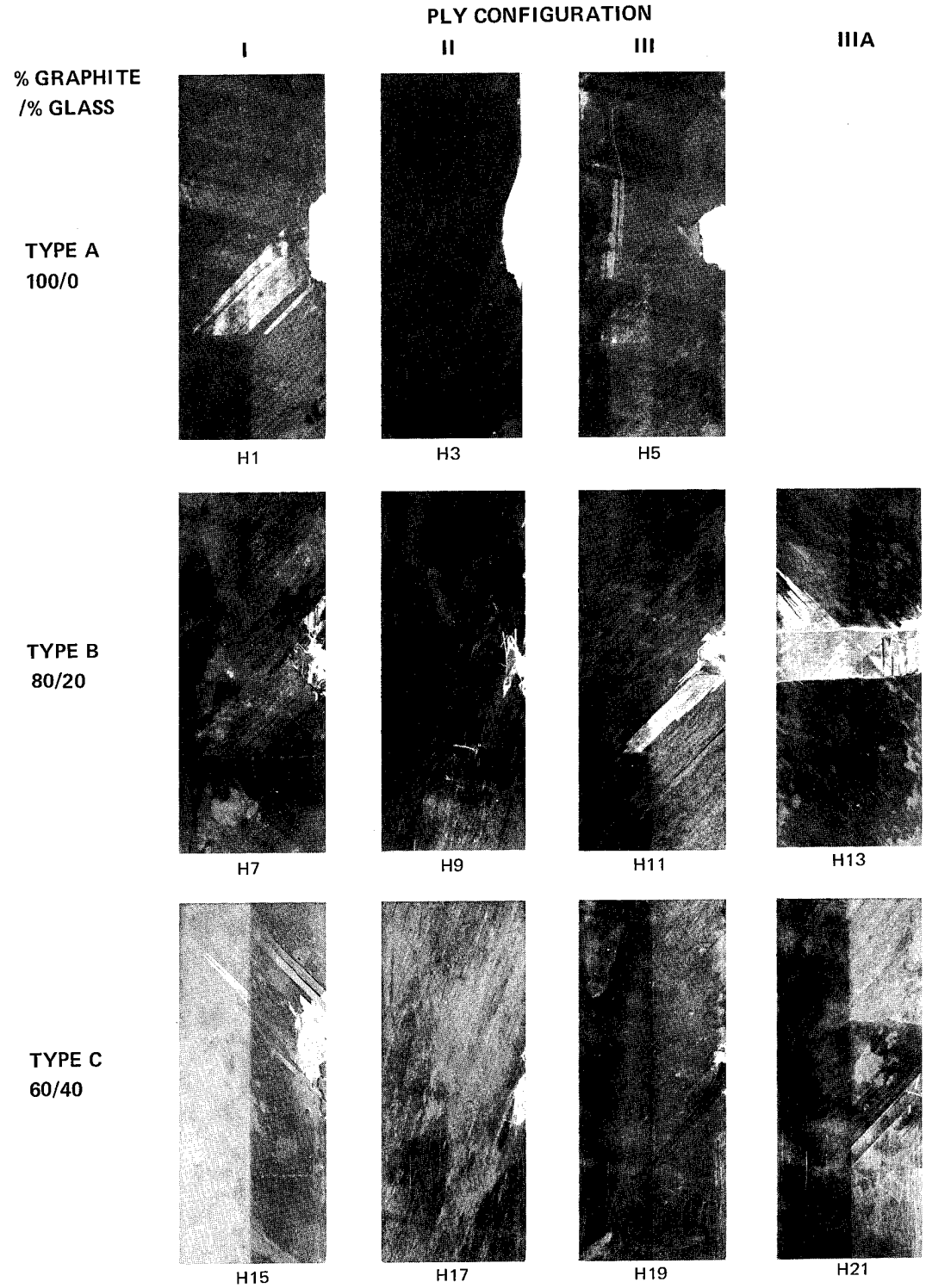

Figure 15 Impacted Composite Blades Showing Damage to the Back Face From a 2.54 cm Diameter Gelatin Ball at a Velocity of 150 m/sec and 30° to the Blade Chord

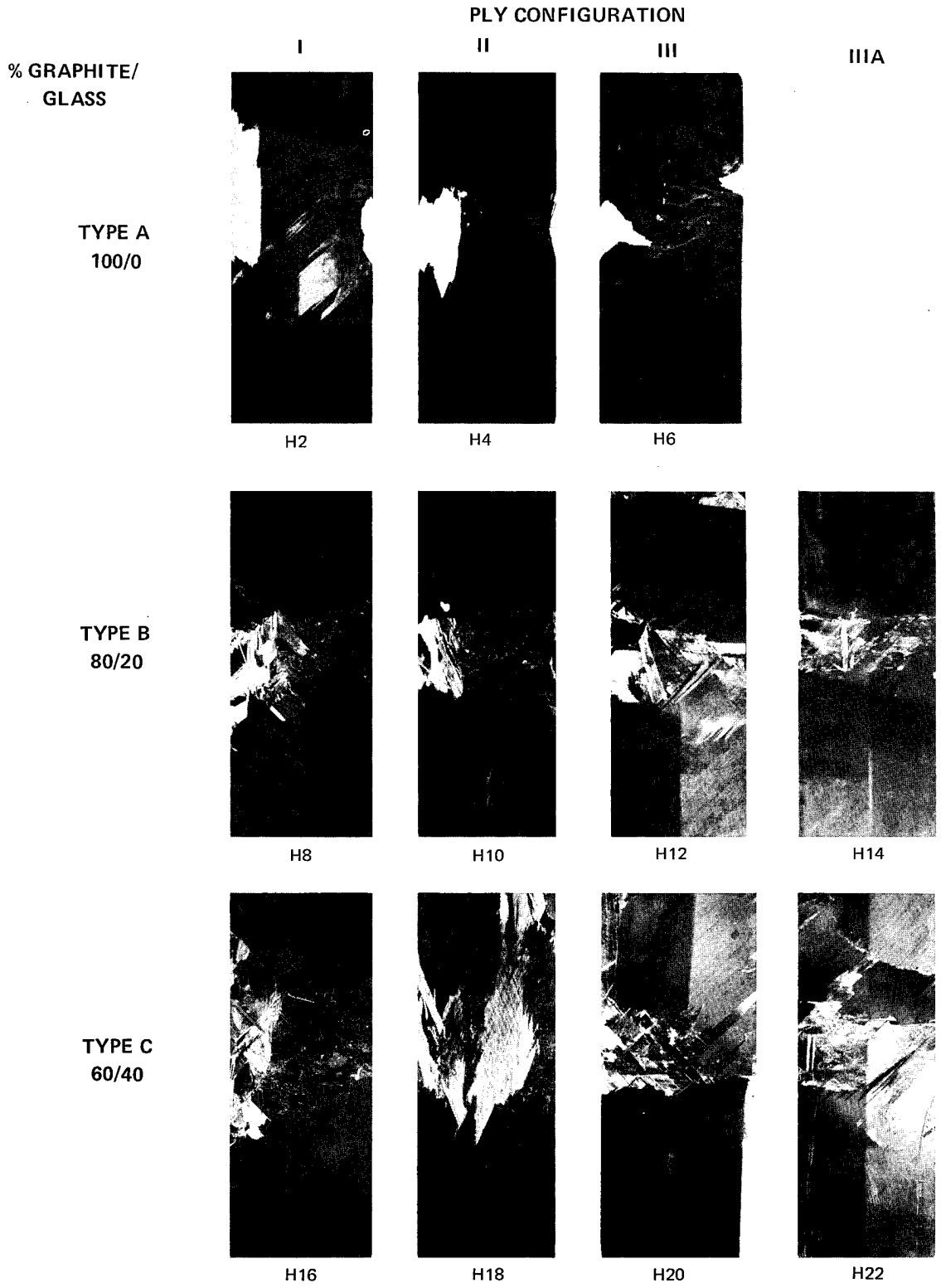

Figure 16 Impacted Composite Blades Showing Damage to the Back Face From a 2.54 cm Diameter Gelatin Ball at a Velocity of 275 m/sec and 30° to the Blade Chord. The Left Edge is the Impact Face. Damage to the Right Edge is From a Prior Impact at 90 m/sec.

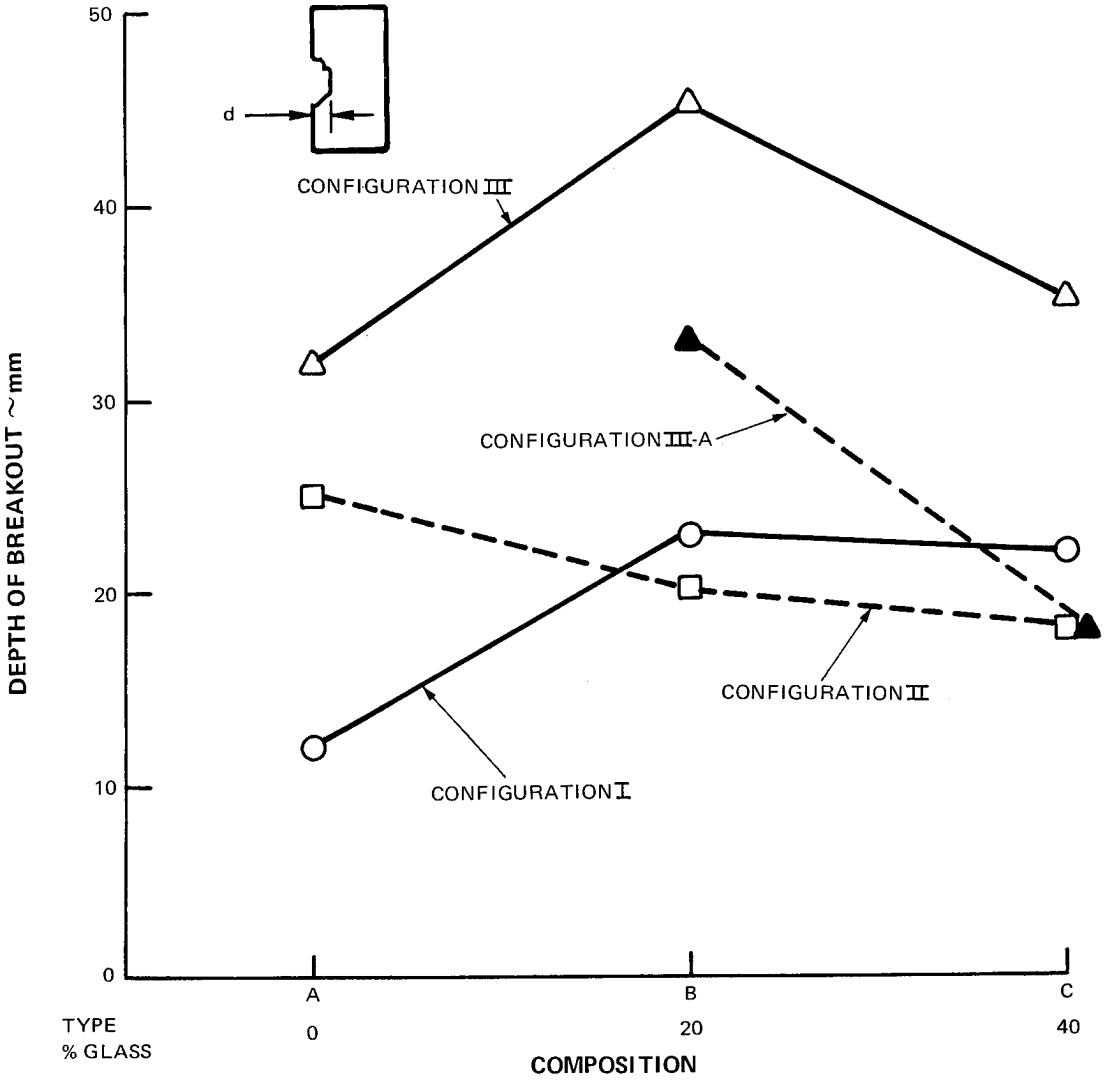

Figure 17 Depth of Damage Region at Leading Edge in Blades After Impact at 275 m/sec. Glass Content Has Limited Effect

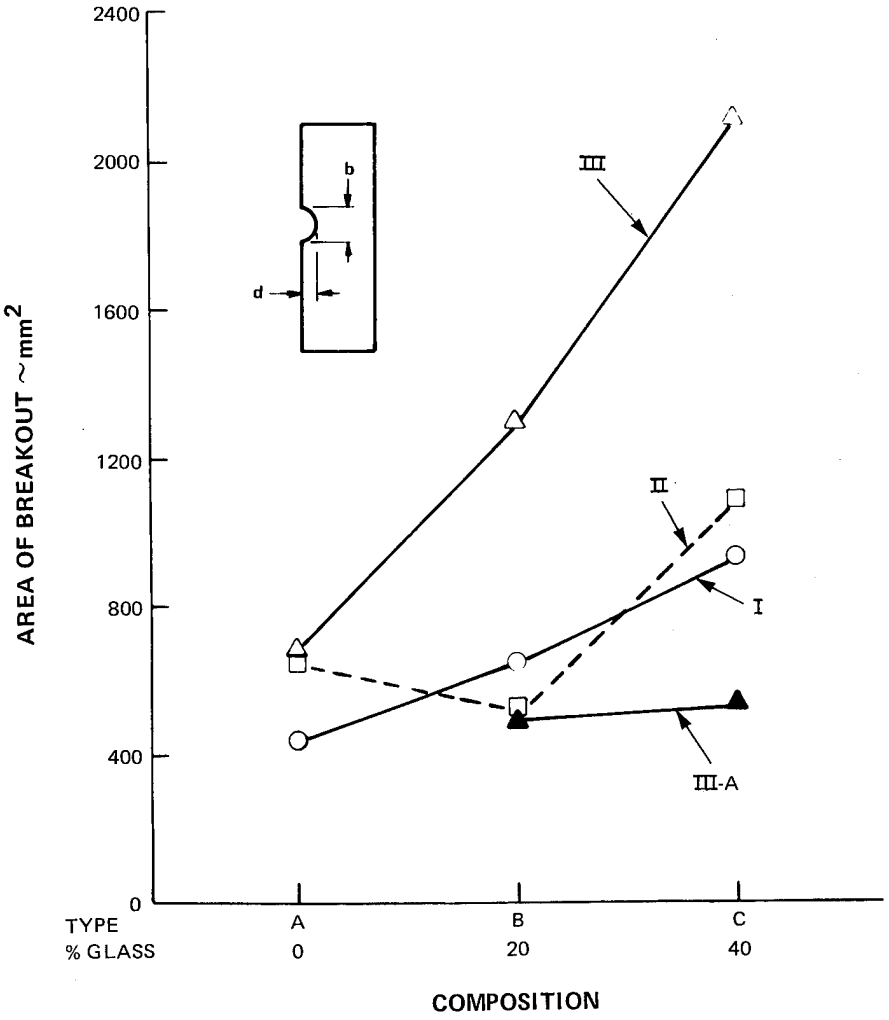

Figure 18 Area of Material Loss at Leading Edge in Blades After Impact at 275 m/sec. Glass Content Increases Area of Damage by Extending the Damage Along the Leading Edge

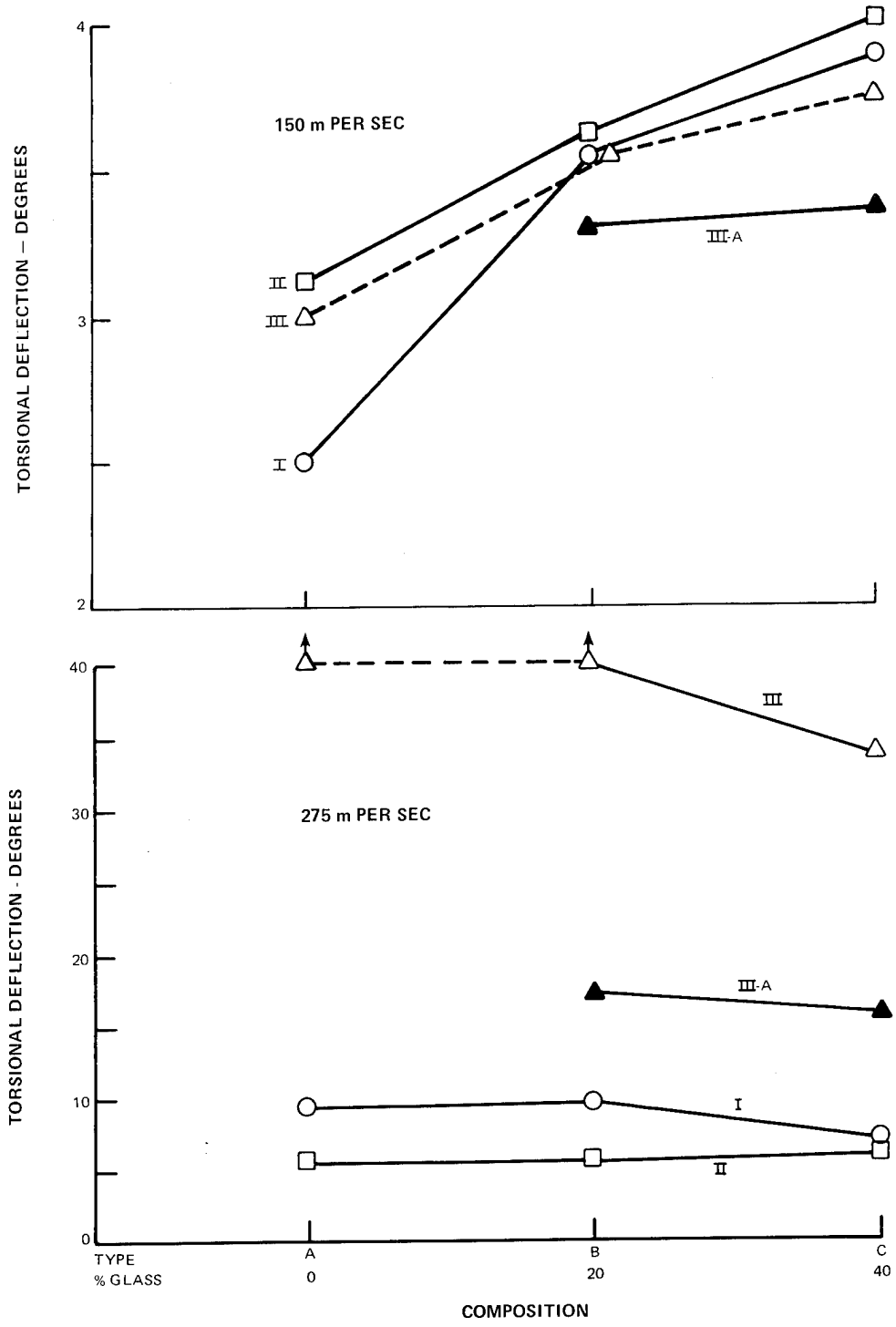

Figure 19 Torsional Deflection of Blades Impacted at 150 m/sec, Where They Were Lightly Damaged, and 275 m/sec, Where Heavier Damage Was Incurred. Torsional Load Was 425 Newton-Meters

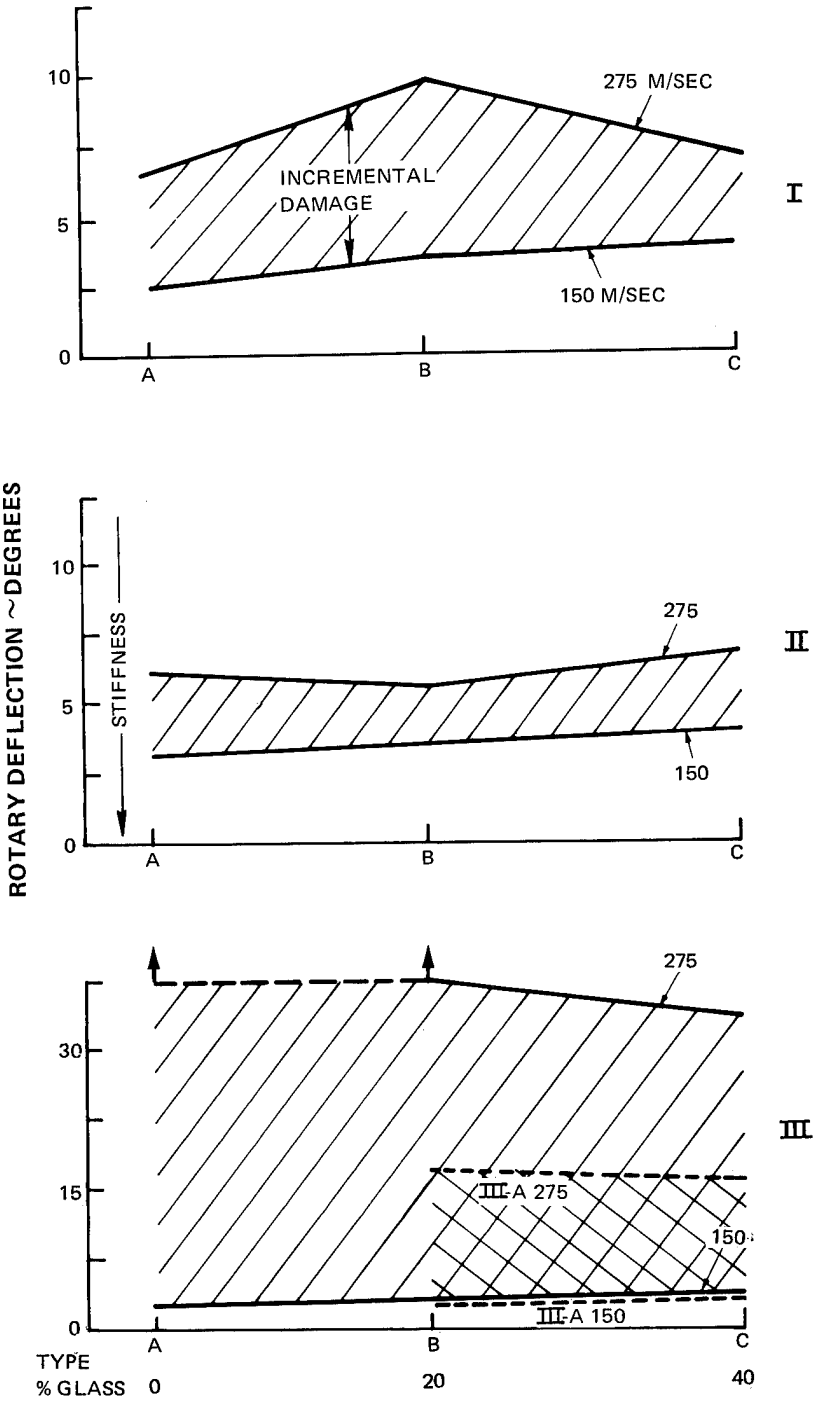

Figure 20 Change in Torsional Rigidity in Blades After Impacting. Torsional Load was 425 Newton-Meters. The Effect of Ply Orientation is Greater Than the Effect of Glass Content

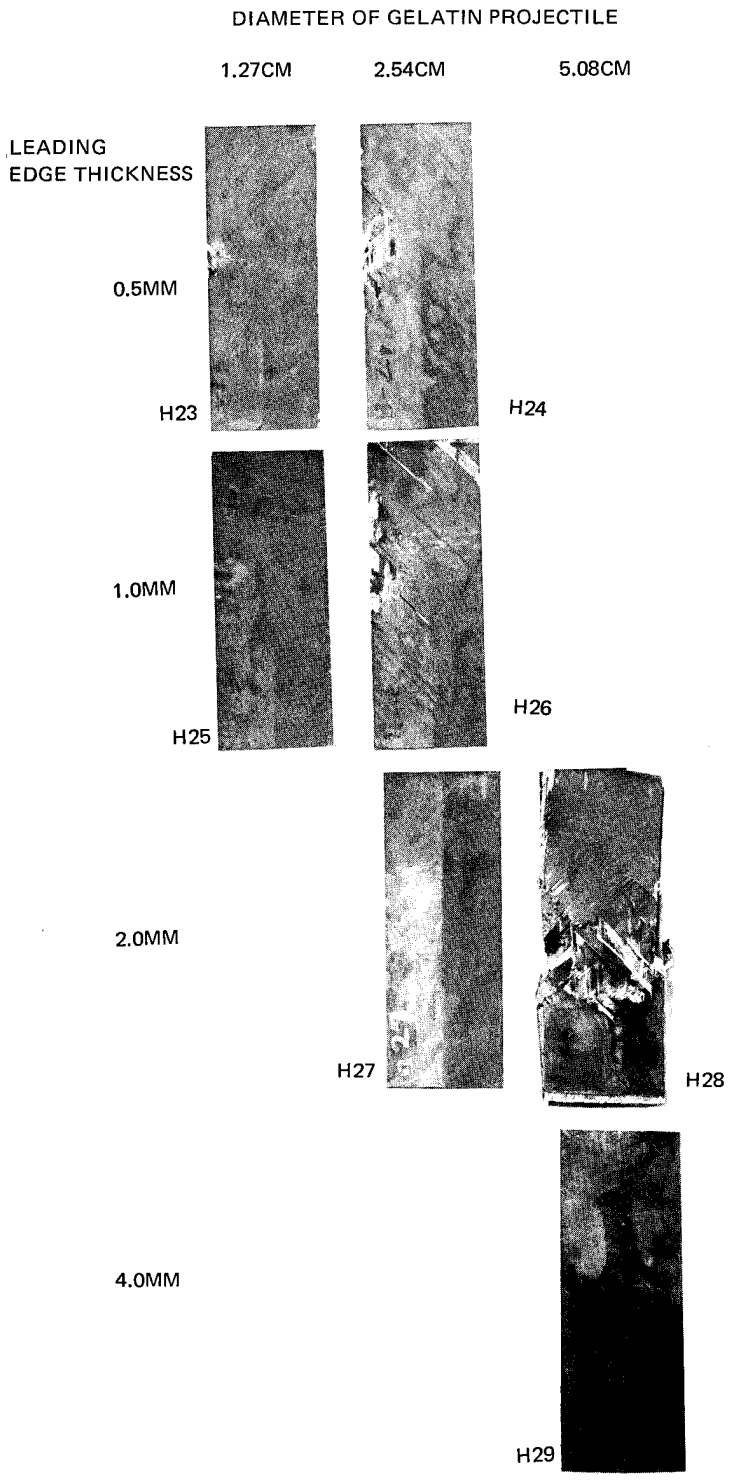

Figure 21 Damage to the Impact Face of Varying Thickness S-Glass + Graphite/Epoxy Composite Blades After Impact with Gelatin Projectiles at 275 m/sec and 30° to the Blade Chord

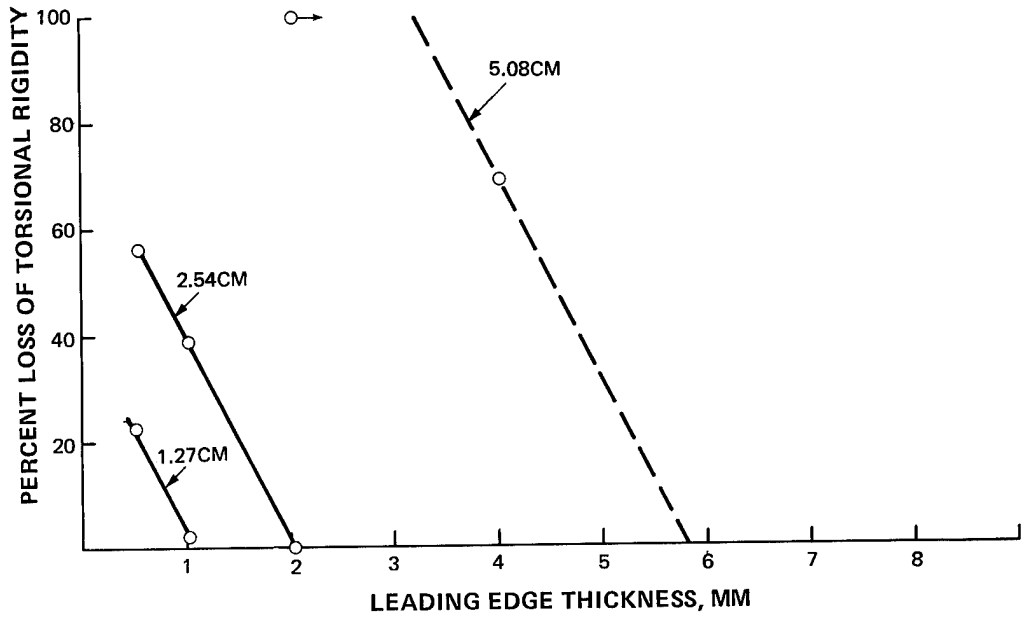

Figure 22 Blade Damage vs. Blade Thickness for Gelatin Projectile Impacts at 275 m/sec on S-Glass + Graphite/Epoxy Blades

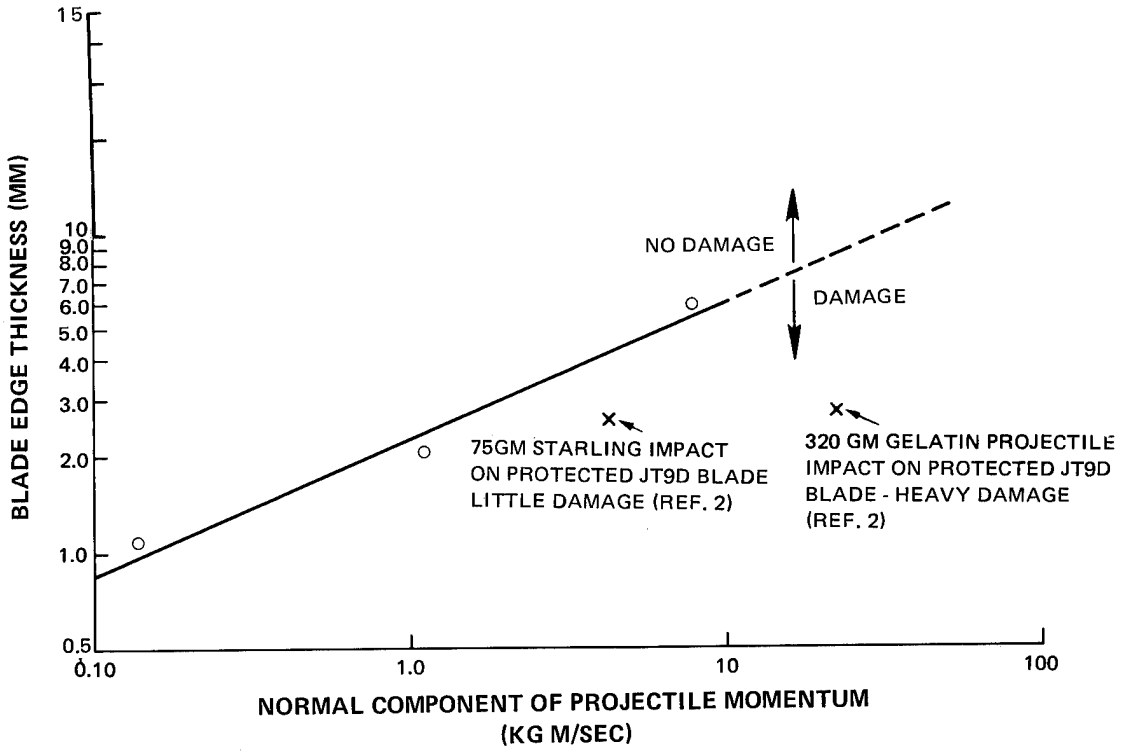

Figure 23 Hybrid Blade Thickness Required to Prevent Impact Damage as a Function of Normal Component of Foreign Object Momentum

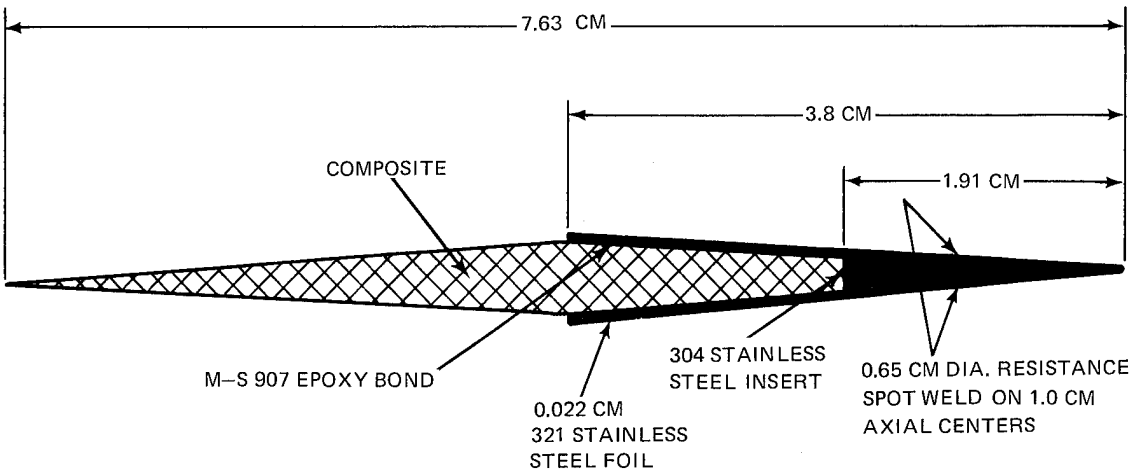

Figure 24 Cross Section View Showing Simulated Blade Specimen with Leading Edge Protection

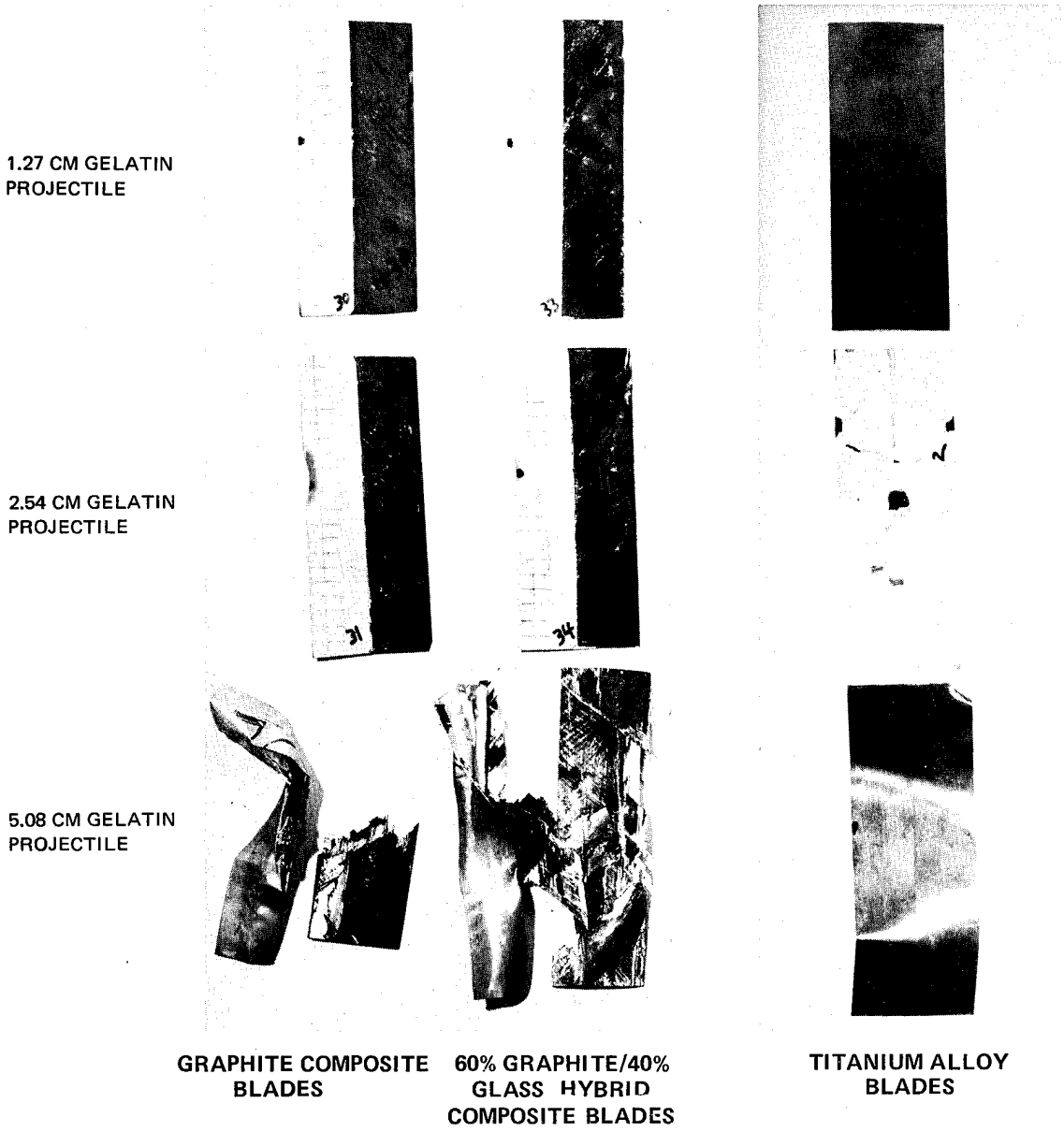

Figure 25 Gelatin Projectile Impact Test Results of Protected Composite and Titanium Alloy Simulated Blades (1.27 and 2.54 cm Gelatin Projectile - 275 m/sec - 30° to Blade Chord) (5.08 cm Gelatin Projectile - 245 m/sec - 30° to Blade Chord)

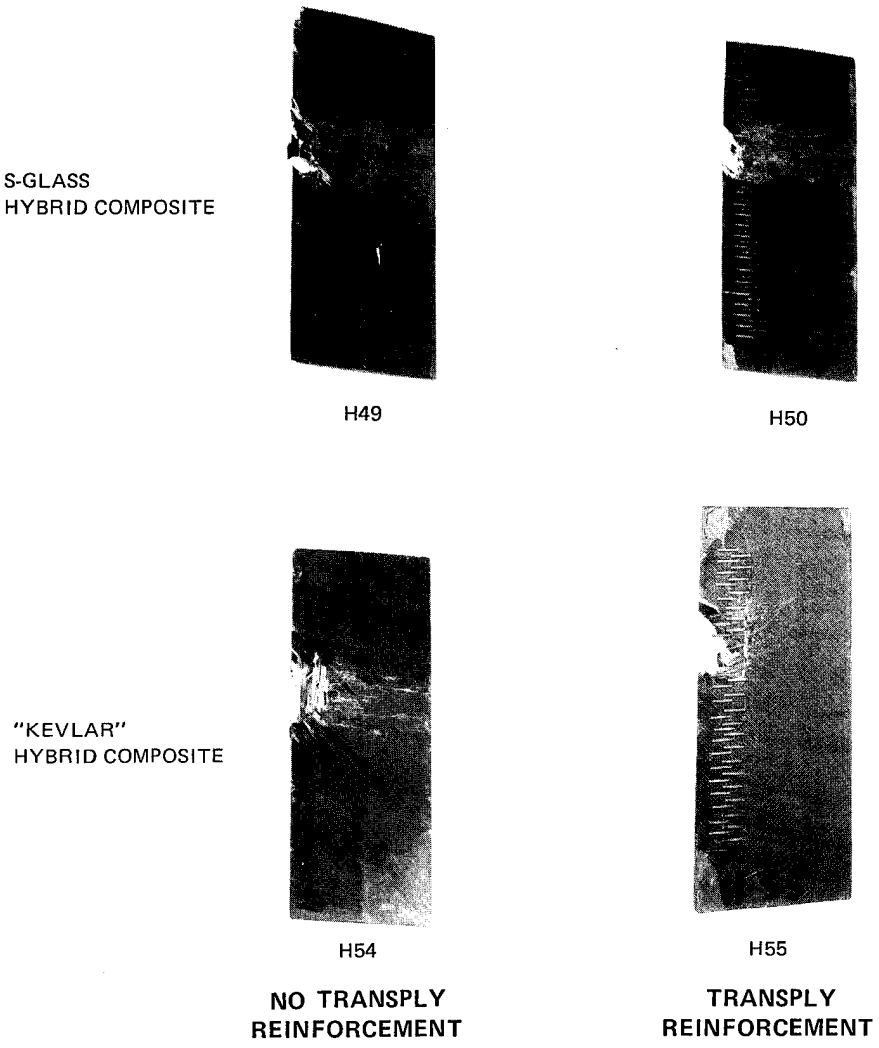

Figure 26 Effect of Trans-Ply Reinforcement on Ballistic Impact Resistance of Hybrid Composite Blades (2.54 cm Gelatin Projectile - 275 m/sec - 30° to Blade Chord)

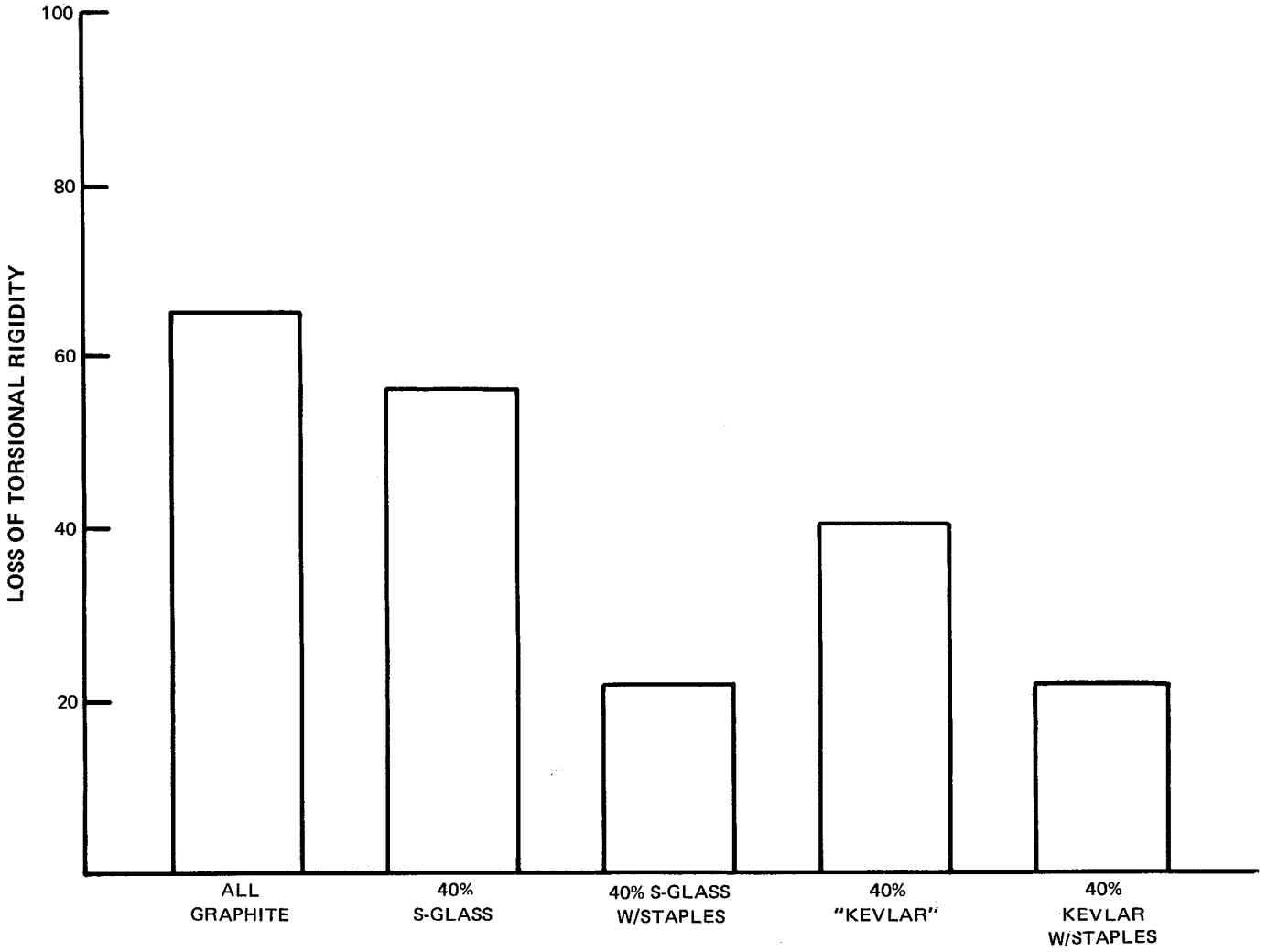

Figure 27 Loss of Torsional Rigidity for Blade Specimens Impacted with 2.54 cm Diameter Gelatin at 275 m/sec 30° to the Blade Chord

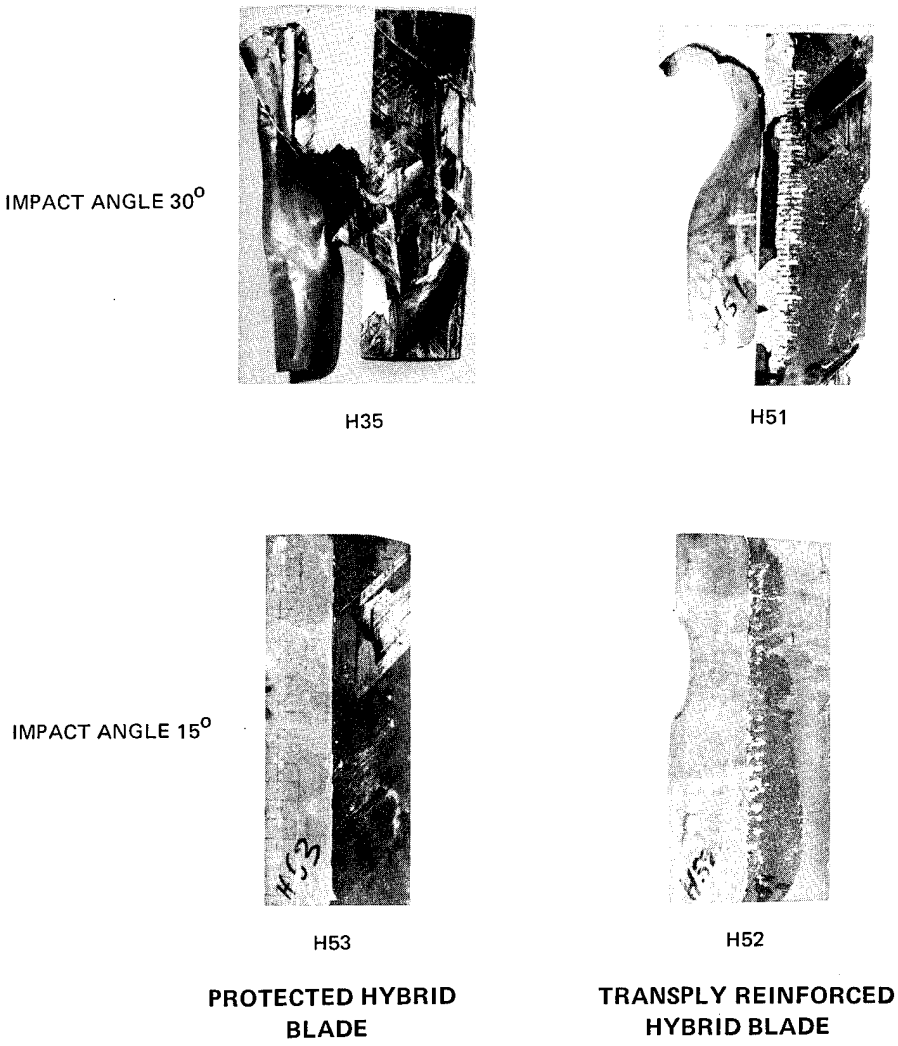

Figure 28 Effect of Trans-Ply Reinforcement on Ballistic Impact Resistance of Protected Hybrid Composite Blades

Figure 29 Results of Spin Impact Testing of Hybrid Composite and Titanium Alloy Simulated Blades

VI. DISTRIBUTION LIST

NASA-Lewis Research Center
21000 Brookpark Rd.
Cleveland, OH 44135
Attn: Contract Section B, MS 500-313
Patent Counsel, MS 500-113
Tech. Util. Office, MS 3-19
AFSC Liaison Office, MS 501-3
AAMRDL Office, MS 500-317
Report Control Office, MS 5-5
Library, MS 60-3 (2 copies)
G. M. Ault, MS 3-5
R. W. Hall, MS 49-1
J. C. Freche, MS 49-1
R. H. Kemp, MS 49-3
R. H. Johns, MS 49-3 (25 copies)
T. D. Gulko, MS 49-3
N. T. Saunders, MS 105-1
M. P. Hanson, MS 501-7
T. T. Serafini, MS 49-1
R. A. Signorelli, MS 106-1
C. C. Chamis, MS 49-3
R. F. Lark, MS 49-3
J. R. Faddoul, MS 49-3

NASA Scientific and Technical Information Facility
P. O. Box 33
College Park, MD 20740
Attn: Acquisitions Branch (10 copies)

NASA Headquarters
Washington, DC 20546
Attn: G. C. Deutsch

NASA-Langley Research Center
Hampton, VA 23365
Attn: Library

NASA-George C. Marshall Space Flight Center
Huntsville, AL 35812
Attn: Library

Air Force Flight Dynamics Laboratory
Wright-Patterson Air Force Base, OH 45433
Attn: C. D. Wallace (FBC)
P. A. Parmley

Defense Metals Information Center
Battelle Memorial Institute
Columbus Laboratories
505 King Ave.
Columbus, OH 43201

Department of the Army
U. S. Army Material Command
Washington, DC 20315
Attn: AMCRD-RC

Department of the Army
U. S. Army Aviation Materials Laboratory
Fort Eustis, VA 23604
Attn: Library

Department of the Army
U. S. Army Aviation Systems Command
P. O. Box 209
St. Louis, MO 63166
Attn: Library

U. S. Army Materials and Mechanics Research Center
Watertown Arsenal
Watertown, MA 02192
Attn: Library

Department of the Army
Watervliet Arsenal
Watervliet, NY 12189
Attn: Library

Department of the Army
Plastics Technical Evaluation Center
Picatinny Arsenal
Dover, NJ 07801
Attn: H. E. Pebly, Jr.

E. I. duPont deNemours and Co., Inc.
Experimental Station
Wilmington, DE 19898
Attn: E. A. Merriman (Dr.)

General Technologies Corp.
1821 Michael Faraday Dr.
Reston, VA 22070
Attn: R. G. Shaver (Dr.)
Vice Pres., Engineering

Douglas Aircraft Co.
3855 Lakewood Blvd.
Long Beach, CA 90801
Attn: L. Rochte
R. Kawai

Union Carbide Corp.
Carbon Products Division
P. O. Box 6116
Cleveland, OH 44101
Attn: J. C. Bowman

Department of the Navy
Office of Naval Research
Washington, DC 20360
Attn: Library

Director
Naval Research Laboratory
Washington, DC 20390

Commander
Naval Air Systems Command
Washington, DC 20360

Commander
Naval Ordnance Systems Command
Washington, DC 20360

Department of the Navy
U. S. Naval Ship R&D Laboratory
Annapolis, MD 21402
Attn: Library

Naval Ship Systems Command
Code 03423
Washington, DC 20360
Attn: C. H. Pohler

National Science Foundation
Engineering Division
1800 G. St., NW
Washington, DC 20540
Attn: Library

U. S. Naval Ordnance Laboratory
White Oak
Silver Spring, MD 20910
Attn: F. R. Barnet

General Dynamics
Convair Aerospace Division
Ft. Worth Operation
P. O. Box 738
Ft. Worth, TX 76101
Attn: Manufacturing Engineering Technical
Library, MZ 62112

General Dynamics
Convair Aerospace Division
San Diego, CA 92112
Attn: J. Haskins (Dr.)

Materials Sciences Corp.
1777 Walton Rd.
Blue Bell, PA 19422
Attn: B. W. Rosen (Dr.)

E. I. duPont deNemours and Co., Inc.
1007 Market St.
Wilmington, DE 19808
Attn: C. H. Zweben (Dr.)
Bldg. 262, Rm. 433

Structural Composites Industries, Inc.
6344 North Irwindale Ave.
Azusa, CA 91702
Attn: E. E. Morris

AiResearch Division
Garrett Corp.
9851 Sepulveda Blvd.
Los Angeles, CA 90009
Attn: Library

Fiber Science, Inc.
245 East 157th St.
Gardena, CA 90248
Attn: L. J. Ashton

United Aircraft Research Laboratories
United Aircraft Corp.
East Hartford, CT 06108
Attn: M. DeCrescente (Dr.)

Hamilton Standard Division
United Aircraft Corp.
Windsor Locks, CT 06096
Attn: A. Jackson

General Electric Co.
Aircraft Engine Group
Evendale, OH 45215
Attn: C. A. Steinhagen
M. Grandy
C. Salemme

General Electric Co.
Lynn River Works
1000 Western Ave.
Lynn, MA 01910
Attn: F. Erich, MS 34505

General Electric Co.
Corporate Research and Development Center
1 River Rd.
Schnectady, NY
Attn: S. Levy

TRW, Inc.
23555 Euclid Ave.
Cleveland, OH
Attn: W. E. Winters

Bell Aerospace
Division of Textron
Buffalo, NY 14240
Attn: Library

Illinois Institute of Technology
10 West 32nd St.
Chicago, IL 60616
Attn: L. J. Broutman (Prof.)

Purdue University
West Lafayette, IN
Attn: C. T. Sun (Prof.)

Drexel University
Philadelphia, PA
Attn: P. C. Chau (Prof.)

Northwestern University
Evanston, IL
Attn: J. D. Achenbach (Prof.)

Hercules, Inc.
Wilmington, DE 19899
Attn: G. C. Kuebeler

University of Florida
Gainesville, FL
Attn: G. Nevill (Prof.)
R. L. Sierakowski (Prof.)

George Washington University
St. Louis, MO 63130
Attn: E. M. Wu (Prof.)

Grumman Aerospace Corp.
S. Oyster Bay Rd.
Bethpage, Long Island, NY 11714
Attn: R. N. Hadcock

North American Aviation Division
Rockwell, Inc.
International Airport
Los Angeles, CA 90009
Attn: J. Ford

Hughes Aircraft Co.
Aerospace Group
Culver City, CA 90230
Attn: R. W. Jones (Dr.), MS D132

Lockheed Co.
Burbank, CA
Attn: T. Higgins

Lockheed-Georgia Co.
Marietta, GA 30060
Attn: H. S. Sweet

Goodyear Aerospace Corp.
1210 Massilon Rd.
Akron, OH 44315
Attn: G. L. Jeppesen

Vertol Division
The Boeing Co.
Philadelphia, PA 19142
Attn: R. A. Pinckney

Whittaker Corp.
Research and Development Center
3540 Aero Ct.
San Diego, CA 92123
Attn: R. K. Berg (Dr.)

Southwest Research Institute
8500 Culebra Rd.
San Antonio, TX 78284
Attn: G. C. Grimes

IITRI
10 West 35th St.
Chicago, IL 60616
Attn: I. M. Daniel (Dr.)

Lawrence Livermore Laboratory
University of California
P. O. Box 808, L-421
Livermore, CA 94550
Attn: T. T. Chiao

Boeing Aerospace Co.
P. O. Box 3999
Seattle, WA 98124
Attn: H. Higgins

Boeing Co.
Wichita Division
Wichita, KS 67210
Attn: D. Torkelson

Martin-Marietta Corp.
Denver, CO
Attn: A. Holston

Battelle Memorial Institute
505 King Ave.
Columbus, OH 43201
Attn: L. E. Hulbert (Dr.)

Babcock and Wilcox Co.
Advanced Composites Department
P. O. Box 419
Alliance, OH 44601
Attn: R. C. Young

National Bureau of Standards
Engineering Mechanics Section
Washington, DC 20234
Attn: R. Mitchell (Dr.)

University of Dayton Research Institute
Dayton, OH 45409
Attn: F. K. Bogner (Dr.)

Detroit Diesel-Allison Division
General Motors Corp.
Indianapolis, IN
Attn: M. Herman (Dr.)

Sikorsky Aircraft Division
United Aircraft Corp.
Stratford, CT 06602
Attn: M. Salkind (Dr.)

Princeton University
Department of Aerospace and Mechanical Sciences
Forrestal Campus
Princeton, NJ 08540
Attn: F. C. Moon (Dr.)

Aluminum Company of America
1200 Ring Building
Washington, DC 20036
Attn: G. B. Barthold

Teledyne-CAE
1330 Laskey Rd.
Toledo, OH 43601

Rohr Corp.
Box 878
Foot and H Sts.
Chula Vista, CA
Attn: F. Hom

Ling-Temco-Vought, Inc.
P. O. Box 6267
Dallas, TX 75222
Attn: N. W. Tillinghost

Grumman Aerospace Corp.
South Oyster Bay Rd.
Bethpage, NY 11714
Attn: C. Hoeltzer

Lycoming Division
AVCO Corp.
550 S. Main St.
Stratford, CT 06497
Attn: H. Jordan

Aerospace, Inc.
2350 E. El Segundo Blvd.
El Segundo, CA 90045
Attn: E. Hinz

NASA-Lyndon B. Johnson Space Center
Houston, TX 77001
Attn: Library

NASA-Ames Research Center
Moffett Field, CA 94035
Attn: Library

NASA-Flight Research Center
P. O. Box 273
Edwards, CA 93523
Attn: Library

NASA-Goddard Space Flight Center
Greenbelt, MD 20771
Attn: Library

Jet Propulsion Laboratory
4800 Oak Grove Dr.
Pasadena, CA 91103
Attn: Library

Advanced Research Projects Agency
Washington, DC 20525
Attn: Library

Air Force Office of Scientific Research
Washington, DC 20333
Attn: Library

Air Force Materials Laboratory
Wright-Patterson Air Force Base, OH 45433
Attn: MBM/S. Tsai (Dr.)
LTN/J. D. Ray
MBC/T. J. Reinhart
MXE/J. Rhodehamel
MBC/C. E. Husman
LLN/A. Hopkins (Dr.)

Air Force Aeronautical Propulsion Laboratory
Wright-Patterson Air Force Base, OH 45433
Attn: TBP/L. J. Obery
CA/Heiser (Dr.)
TBP/T. Norbut

Commander
Aberdeen Proving Ground
Aberdeen Proving Ground, MD 21005
Attn: STEAP-TL, Bldg. 305, Mrs. Patchell